

Exponent[®]

Mechanics and Materials Practice

**BN64159
Comparison of Selected
Lithium-Ion Battery
Chemistries**

Testing Report

July 11, 2007



BN64159
**Comparison of Selected Lithium-
Ion Battery Chemistries**

Testing Report

Prepared for

Eileen S. Saidi, Ph.D.
Director of Applied Research
Valence Technology Inc.
1889 E. Maule Ave, Suite A
Las Vegas, NV 89119

Prepared by

Noah Budiansky, Ph.D.
Quinn Horn, Ph.D.
Xiaoyun Hu
Kevin White, Ph.D.
Exponent
21 Strathmore Road
Natick, MA 01760

July 11, 2007

© Exponent, Inc.

BN64159-D0F0-0707-R003

Contents

	<u>Page</u>
List of Figures	2
List of Tables	6
Executive Summary	7
1. Crush Test	11
Test Purpose	11
Test Setup	11
Test Results	13
Test Summary	32
2. Heating Test	34
Test Purpose	34
Test Setup	34
Test Results	39
Test Summary	52
3. Accelerating Rate Calorimetry	54
Test Purpose	54
Methods	54
Results	55
Test Summary	70

List of Figures

	<u>Page</u>
Figure 1. Schematic of crush test apparatus.	12
Figure 2. Photograph of crush test apparatus positioned in lab press.	13
Figure 3. $\text{Li}(\text{Co}_{1/3}\text{Ni}_{1/3}\text{Mn}_{1/3})\text{O}_2$ cell 2007964 voltage and temperature profile during crush test.	14
Figure 4. $\text{Li}(\text{Co}_{1/3}\text{Ni}_{1/3}\text{Mn}_{1/3})\text{O}_2$ cell 2002828 voltage and temperature profile during crush test.	14
Figure 5. $\text{Li}(\text{Co}_{1/3}\text{Ni}_{1/3}\text{Mn}_{1/3})\text{O}_2$ cell 2006711 voltage and temperature profile during crush test.	15
Figure 6. LiCoO_2 cell 1008751 voltage and temperature profile during crush test.	15
Figure 7. LiCoO_2 cell 1008750 voltage and temperature profile during crush test.	16
Figure 8. LiCoO_2 cell 1008736 voltage and temperature profile during crush test.	16
Figure 9. LiCoO_2 cell 1012155 voltage and temperature profile during crush test.	17
Figure 10. Valence phosphate cell 15930855 voltage and temperature profile during crush test.	17
Figure 11. Valence phosphate cell 15927928 voltage and temperature profile during crush test.	18
Figure 12. Valence phosphate cell 15929364 voltage and temperature profile during crush test.	18
Figure 13. Summary of peak cell skin temperature during crush test. Error bars indicate one standard deviation from the mean.	21
Figure 14. Average cell weight losses after crush testing. Error bars indicate range of weight loss.	22
Figure 15. Post crush test X-ray image of $\text{Li}(\text{Co}_{1/3}\text{Ni}_{1/3}\text{Mn}_{1/3})\text{O}_2$ cell 2007964.	23
Figure 16. Post crush test X-ray image of $\text{Li}(\text{Co}_{1/3}\text{Ni}_{1/3}\text{Mn}_{1/3})\text{O}_2$ cell 2002828.	24
Figure 17. Post crush test X-ray image of $\text{Li}(\text{Co}_{1/3}\text{Ni}_{1/3}\text{Mn}_{1/3})\text{O}_2$ cell 2006711.	25
Figure 18. Post crush test X-ray image of LiCoO_2 cell 1008751.	26
Figure 19. Post crush test X-ray image of LiCoO_2 cell 1008750.	27
Figure 20. Post crush test X-ray image of LiCoO_2 cell 1008736.	28

Figure 21.	Post crush test X-ray image of LiCoO ₂ cell 1012155.	29
Figure 22.	Post crush test X-ray image of phosphate cell 15930855.	30
Figure 23.	Post crush test X-ray image of phosphate cell 15927928.	31
Figure 24.	Post crush test X-ray image of phosphate cell 15929364.	32
Figure 25.	a) Schematic break down of heat test apparatus. b) Underneath the protective covering layer insulation was used to prevent radiative heat loss from the c) heat tape wrapped around the center heater tube. d) The temperature of the test apparatus was monitored with a J-type thermocouple located between the heating tape and the center heater tube. Bolts located near both ends of the cell prevent the cell from being ejected when the cell vented.	36
Figure 26.	Photograph of heat test apparatus.	37
Figure 27.	Photograph of heat test apparatus supported in laboratory press for testing.	37
Figure 28.	Exemplar commercial lithium mixed oxide cell pre-test X-ray.	38
Figure 29.	Exemplar commercial lithium cobalt oxide cell pre-test X-ray.	38
Figure 30.	Exemplar Valence phosphate cell pre-test X-ray.	39
Figure 31.	Li(Co _{1/3} Ni _{1/3} Mn _{1/3})O ₂ cell 2007149 voltage and temperature profile during heat test.	40
Figure 32.	Li(Co _{1/3} Ni _{1/3} Mn _{1/3})O ₂ cell 2007023 voltage and temperature profile during heat test.	40
Figure 33.	Li(Co _{1/3} Ni _{1/3} Mn _{1/3})O ₂ cell 2001015 voltage and temperature profile.	41
Figure 34.	LiCoO ₂ cell 1012133 voltage and temperature profile during heat test.	41
Figure 35.	LiCoO ₂ cell 1008815 voltage and temperature profile during heat test.	42
Figure 36.	LiCoO ₂ cell 1012144 voltage and temperature profile during heat test.	42
Figure 37.	Phosphate cell 15930325 voltage and temperature profile during heat test.	43
Figure 38.	Phosphate cell 15929411 voltage and temperature profile during heat test.	43
Figure 39.	Phosphate cell 15927964 voltage and temperature profile during heat test.	44
Figure 40.	Summary of cell skin temperature during heating test. Error bars indicate the range of values measured.	47
Figure 41.	Post heating test X-ray image of Li(Co _{1/3} Ni _{1/3} Mn _{1/3})O ₂ cell 2007149.	48
Figure 42.	Post heating test X-ray image of Li(Co _{1/3} Ni _{1/3} Mn _{1/3})O ₂ cell 2007023.	48
Figure 43.	Post heating test X-ray image of Li(Co _{1/3} Ni _{1/3} Mn _{1/3})O ₂ cell 2001015.	49

Figure 44.	Post heating test X-ray image of LiCoO ₂ cell 1012133.	50
Figure 45.	Post heating test X-ray image of LiCoO ₂ cell 1008815.	50
Figure 46.	Post heating test X-ray image of LiCoO ₂ cell 1012144.	51
Figure 47.	Post heating test X-ray image of Valence phosphate cell 15930325.	51
Figure 48.	Post heating test X-ray image of Valence phosphate cell 15929411.	52
Figure 49.	Post heating test X-ray image of Valence phosphate cell 15927964.	52
Figure 50.	Temperature-time profiles of Valence phosphate 18650 cell tested in the open ARC configuration.	56
Figure 51.	Temperature-time profiles of a commercially available lithium cobalt oxide 18650 cell tested in the open ARC configuration.	57
Figure 52.	Temperature-time profiles of a commercially available lithium mixed oxide 18650 cell tested in the open ARC configuration.	57
Figure 53.	Temperature-time and temperature-pressure profiles of Valence phosphate 18650 cell tested in the closed ARC configuration.	58
Figure 54.	Temperature-time and temperature-pressure profiles of a commercially available lithium cobalt oxide 18650 cell tested in the closed ARC configuration.	58
Figure 55.	Temperature-time and temperature-pressure profiles of a commercially available lithium mixed oxide 18650 cell tested in the closed ARC configuration.	59
Figure 56.	Temperature rate as a function of temperature for Valence phosphate 18650 cell tested in the open ARC configuration.	60
Figure 57.	Temperature rate as a function of temperature for a commercially available lithium cobalt oxide 18650 cell tested in the open ARC configuration.	61
Figure 58.	Temperature rate as a function of temperature for commercially available lithium mixed oxide 18650 cell tested in the open ARC configuration.	61
Figure 59.	Temperature rate and pressure rate as a function of temperature for Valence phosphate 18650 cell tested in the closed ARC configuration.	62
Figure 60.	Temperature rate and pressure rate as a function of temperature for a commercially available lithium cobalt oxide 18650 cell tested in the closed ARC configuration.	62
Figure 61.	Temperature rate and pressure rate as a function of temperature for a commercially available lithium mixed oxide 18650 cell tested in the closed ARC configuration.	63

Figure 62. Temperature-time series comparison of Li-ion cell chemistries tested in ARC open configuration.	63
Figure 63. Temperature-time series comparison of Li-ion cell chemistries tested in ARC closed configuration	64
Figure 64. Voltage-time series of Valence phosphate 18650 cell tested in the open ARC configuration. A voltage drop was observed at approximately 150°C corresponding to the time at which breakdown was observed.	65
Figure 65. Voltage-time series of a commercially available lithium cobalt oxide 18650 cell tested in the open ARC configuration. A voltage drop was observed at approximately 120°C corresponding to the time at which breakdown was observed.	65
Figure 66. Voltage-time series of a commercially available lithium mixed oxide 18650 cell tested in the open ARC configuration. A voltage drop was observed at approximately 150°C corresponding to the time at which breakdown was observed.	66
Figure 67. Photograph of Valence phosphate cell after ARC testing in the open configuration.	67
Figure 68. Photograph of Valence phosphate cell after ARC testing in the open calorimeter bomb apparatus.	67
Figure 69. Photograph of a commercially available lithium cobalt oxide 18650 cell after ARC testing in the open cell configuration.	68
Figure 70. Photograph of a commercially available lithium mixed oxide 18650 cell after ARC testing in the open cell configuration.	68
Figure 71. Photograph of Valence phosphate cell after ARC testing in the closed configuration.	69
Figure 72. Photograph of a commercially available lithium cobalt oxide 18650 cell after ARC testing in the closed cell configuration.	69
Figure 73. Photograph of a commercially available lithium mixed oxide 18650 cell after ARC testing in the closed cell configuration.	70

List of Tables

	<u>Page</u>
Table 1. Summary of peak cell skin temperatures during crush testing	20
Table 2. Auto-ignition temperatures for common Li ⁺ electrolytes.	20
Table 3. Summary of cell skin temperature during heat test.	46
Table 4. Accelerating Rate Calorimetry summary results for the open and closed configurations.	59

Executive Summary

The goal of this effort was to characterize the safety-related response of selected lithium-ion chemistries to an intentionally-induced thermal runaway condition. Cells manufactured with three different positive electrode materials were studied: LiCoO_2 , $\text{Li}(\text{Co}_{1/3}\text{Ni}_{1/3}\text{Mn}_{1/3})\text{O}_2$ and phosphate-based materials. The following key results were obtained from the testing conducted on a small number of Valence phosphate 18650 cells in this study:

1. Upon initiation of an internal cell fault by a crush method as described in this report, the Valence phosphate 18650 cells did not reach temperatures sufficiently high to cause melting of the separator, ignition of the electrolyte venting of flames, or ejecting flaming and/or burning debris. In addition, the peak external temperature of the Valence phosphate 18650 cell was more than 100 °C below the temperature required to initiate thermal runaway.
2. Upon initiation of an internal cell fault by an external heating method as described in this report, the peak temperature reached by the Valence phosphate 18650 cells was significantly below cells of other chemistries tested and no ignition of nearby combustible material was observed during venting.
3. During ARC testing by methods described in this report, the Valence phosphate 18650 cells did have a consistently much lower rate of self-heating than cells of other chemistries tested.

Based on these results, it is our opinion that it is unlikely that a single internal cell fault would initiate a propagating thermal runaway in a Valence phosphate battery pack. In addition, the absence of flaming or ejection of burning debris from the Valence phosphate 18650 cells makes it unlikely that material adjacent to the cells could be ignited by a cell suffering from an internal fault. A summary of testing performed on the Valence phosphate 18650 cells, as well as the cells with LiCoO_2 and $\text{Li}(\text{Co}_{1/3}\text{Ni}_{1/3}\text{Mn}_{1/3})\text{O}_2$ cathodes, is presented below.

In order to evaluate the relative safety of lithium-ion cells using these cathode materials, Exponent conducted a series of experiments to measure the following parameters:

1. External temperature of the cell during thermal runaway due to an intentionally induced internal cell fault;
2. Temperature and duration of heating required to initiate thermal runaway under selected conditions;
3. Characteristics of thermal runaway events (e.g. venting, flaming, ejection of debris, etc.);
4. Relative amount of energy produced by electrochemical and chemical reactions during thermal runaway;
5. Rate of temperature increase during thermal runaway.

The temperature of the cells was monitored by affixing thermocouples to individual cells that were subjected to the application of either heat from an external source, or by application of an external force sufficient to crush the cell and induce an internal short circuit. The results of these tests are the subject of this report. Relative amount of energy released and rate of energy release were measured by Accelerating Rate Calorimetry (ARC) at an outside testing laboratory.

The 18650 cells included in the testing were provided to Exponent by Valance and included Valance phosphate (phosphate-based cathode), commercially available lithium cobalt oxide (LiCoO_2 cathode) and commercially available lithium mixed oxide ($\text{Li}(\text{Co}_{1/3}\text{Ni}_{1/3}\text{Mn}_{1/3})\text{O}_2$ cathode) cells. The cells with LiCoO_2 and $\text{Li}(\text{Co}_{1/3}\text{Ni}_{1/3}\text{Mn}_{1/3})\text{O}_2$ cathodes were manufactured by a large lithium-ion battery manufacturer and were considered to be of standard or above average quality. The summary of our findings is as follows:

Crush Tests

- The Valence phosphate cells fail benignly¹ and self-heat to external can temperatures below 115 °C, making spread of thermal runaway to adjacent cells in a battery pack improbable.
- The commercially available lithium mixed oxide cells fail benignly¹ and self-heat to external can temperatures that approach 300 °C. It would be possible for these cells to cause separator shutdown in adjacent cells in a battery and propagate thermal runaway through the pack.
- The commercially available lithium cobalt oxide cells fail violently, with flames external to the cell and self-heat to external can temperatures as high as 543 °C. It would be possible for these cells to cause separator shutdown in adjacent cells in a battery and propagate thermal runaway through the pack.

External Heating Tests

- The temperature at separator shutdown is similar for all of the cells tested. The commercially available lithium mixed oxide cells showed separator shutdown at slightly lower temperature relative to the other two cell types, suggesting a difference in separator chemistry or morphology.
- The temperature at the initiation of thermal runaway was similar for all of the cells tested suggesting a common initiation mechanism.
- The peak metal can skin temperature was substantially higher for the commercially available lithium cobalt oxide and lithium mixed oxide cells relative to the phosphate cells.
- The peak metal can skin temperature of the commercially available lithium cobalt oxide and mixed oxide cells exceeded the auto-ignition temperature for common Li⁺ electrolyte solvents of approximately 450 °C.

¹ A benign cell failure in context of this report does not emit open flames during venting.

- The peak metal can skin temperature of the Valence phosphate cells did not exceed the auto-ignition temperature for the common Li⁺ electrolyte solvents of approximately 450 °C.

Accelerating Rate Calorimetry

- The self-heating onset temperature occurred between 80 °C and 90 °C for all tested cell chemistries. This temperature range is consistent with the breakdown of the secondary solid-electrolyte interface (SEI) layer at the anode.
- The peak temperatures of the metal can skin temperature achieved upon thermal runaway were between 245 °C and 550 °C.
- In both open and closed configurations the Li-ion cell chemistries can be ranked from highest self-heating rate to lowest as follows: commercially available lithium cobalt oxide 18650 cell > commercially available lithium mixed oxide 18650 cell > Valence phosphate 18650 cell.
- Separator shutdown occurs between 120 °C and 150 °C in all the cell chemistries tested.

1. Crush Test

Test Purpose

The purpose of the crush test is to assess the peak cell skin temperatures that can be achieved in the event of an internal short circuit under predefined conditions. These temperatures can then be compared to the thermal runaway temperature of the electrolyte and the initiation temperature for thermal runaway of the electrodes.

Test Setup

Crush tests were performed on cells that were charged to 100% state of charge (SOC) per manufacturers' specifications. Cells were instrumented with high temperature J-type thermocouples mounted on the cell skin at the vent end of the cell and on the cell skin in the center of the cell. The cell potential and the thermocouple voltages were monitored during the duration of the test with a Fluke Hydra data-logging multimeter at a sampling rate of 2 Hz. The ambient temperature was also recorded during the test to ensure that external heating was not a significant contribution to the change in temperature measured at the cell skin.

Cells were positioned in a custom designed cell mount that prevented the cell from rolling when a force was applied to crush the batteries, as shown in Figure 1 and Figure 2. Cells were crushed using a Model 3912 Carver press driving a one-inch diameter hemispherical tipped rod. Increasing force was applied until the cell vented and the thermal event was initiated. The configuration of this crush test is designed to initiate an internal cell fault without damage to the integrity of the crimp/seal assembly as well as breaching the cell case. Crushed cells were allowed to cool in the test apparatus until the cell skin temperature returned to approximately 50 °C.

Cell crush tests were videotaped at a close range to capture the venting of the cell and allow qualitative comparison across the cell chemistries tested. The skin temperature at the center of

the cell and the vent end of the cell, the ambient temperature, and the cell voltage were recorded and reported as temperature and voltage vs. time plots. The peak temperature was reported for all experiments as determined from temperature vs. time plots.

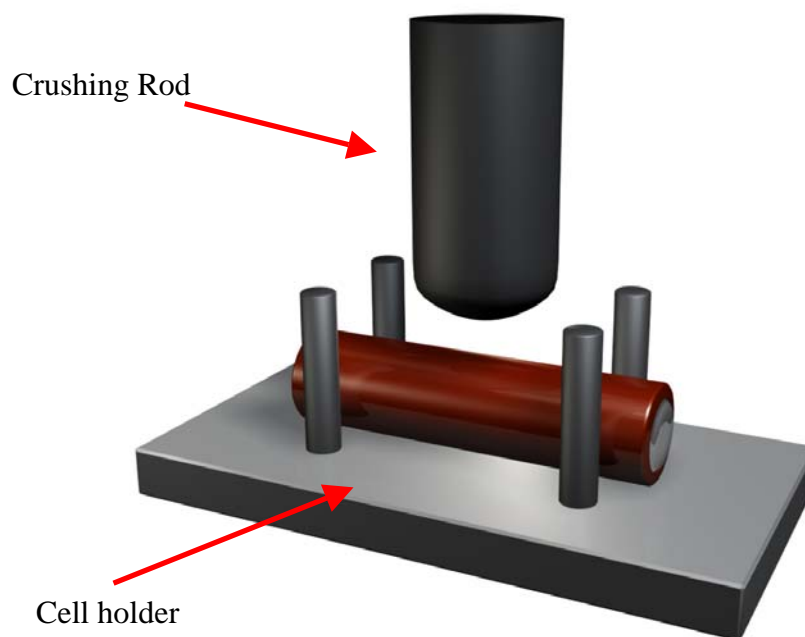


Figure 1. Schematic of crush test apparatus.



Figure 2. Photograph of crush test apparatus positioned in lab press.

Test Results

Figure 3 through Figure 12 show the cell voltage and skin temperature profiles during crush testing. When crushed, the cells all exhibited similar behavior where a rapid increase in temperature was observed that was attributed to physical or chemical changes within the cell:

1. A sudden drop in cell voltage that was attributed to the initiation of the internal cell fault. The physical occurrence is most likely separator rupture due to the applied pressure leading to an internal short circuit.
2. A rapid increase in cell skin temperature that was attributed to internal shorting and the initiation of exothermic chemical reactions that are associated with thermal runaway.

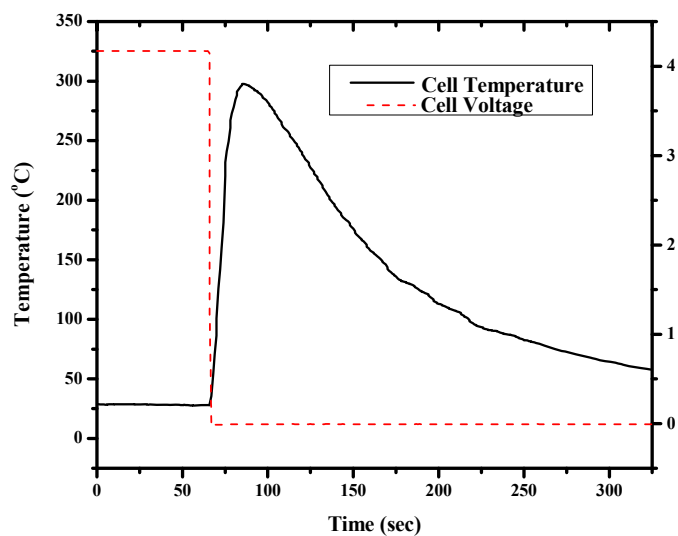


Figure 3. $\text{Li}(\text{Co}_{1/3}\text{Ni}_{1/3}\text{Mn}_{1/3})\text{O}_2$ cell 2007964 voltage and temperature profile during crush test.

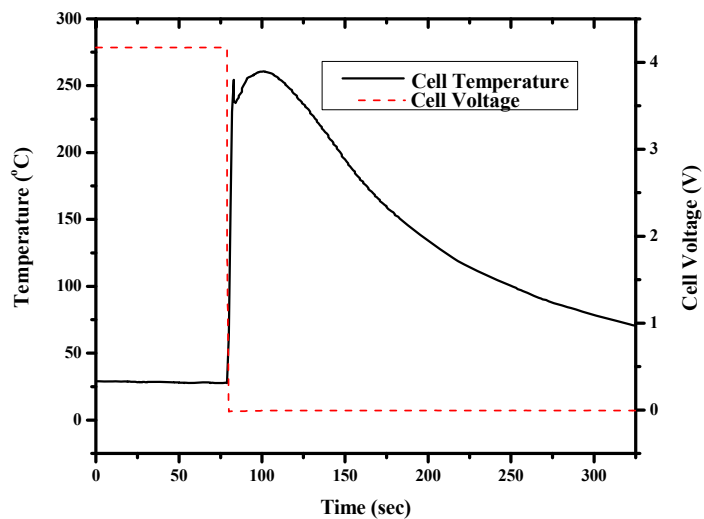


Figure 4. $\text{Li}(\text{Co}_{1/3}\text{Ni}_{1/3}\text{Mn}_{1/3})\text{O}_2$ cell 2002828 voltage and temperature profile during crush test.

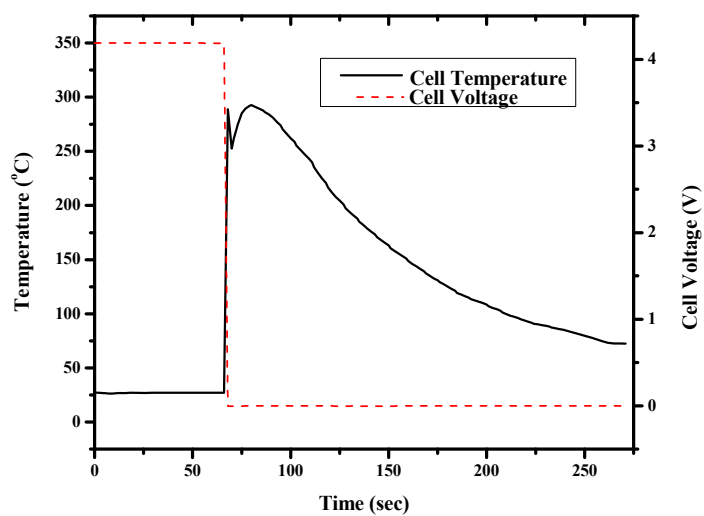


Figure 5. $\text{Li}(\text{Co}_{1/3}\text{Ni}_{1/3}\text{Mn}_{1/3})\text{O}_2$ cell 2006711 voltage and temperature profile during crush test.

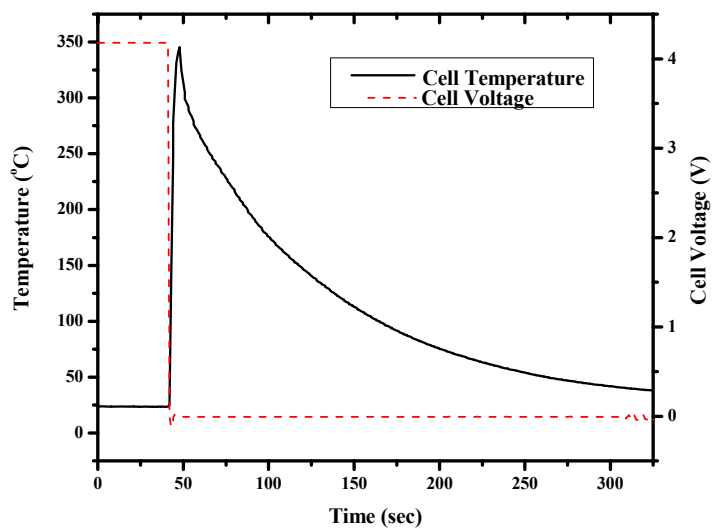


Figure 6. LiCoO_2 cell 1008751 voltage and temperature profile during crush test.

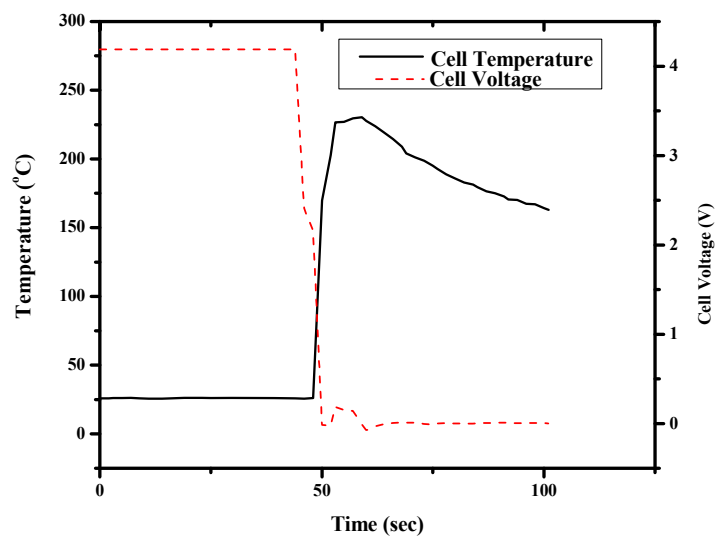


Figure 7. LiCoO₂ cell 1008750 voltage and temperature profile during crush test.

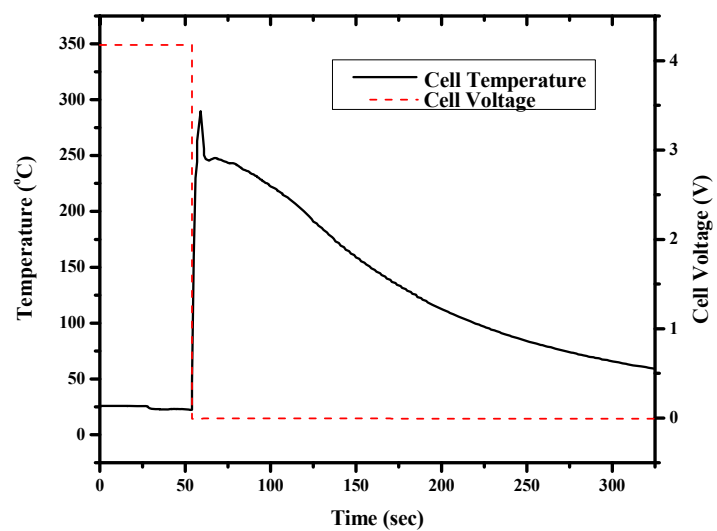


Figure 8. LiCoO₂ cell 1008736 voltage and temperature profile during crush test.

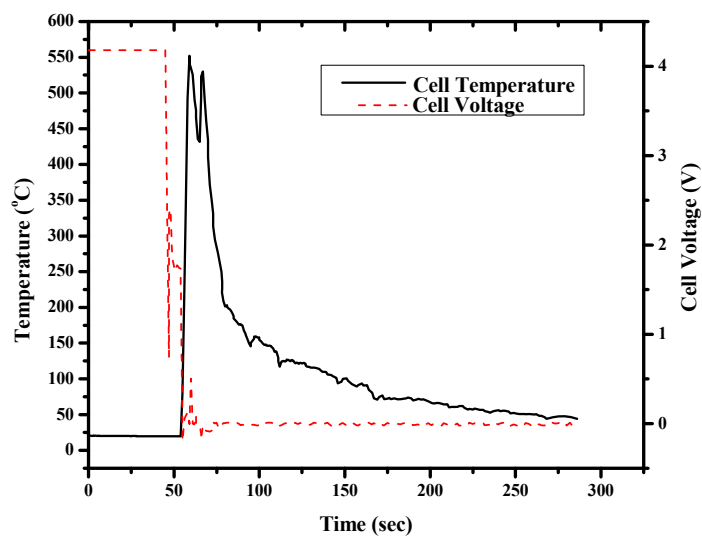


Figure 9. LiCoO₂ cell 1012155 voltage and temperature profile during crush test.

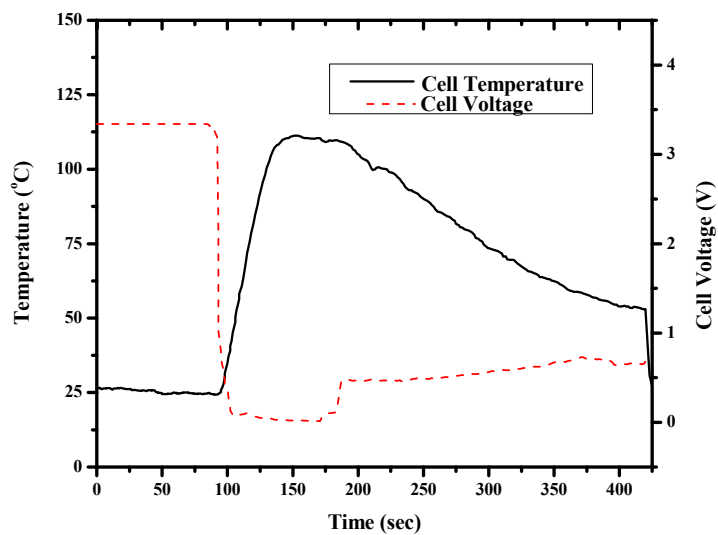


Figure 10. Valence phosphate cell 15930855 voltage and temperature profile during crush test.

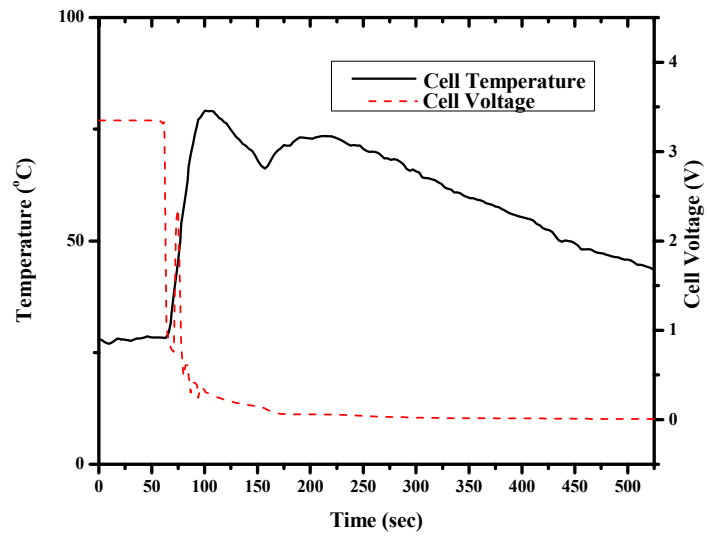


Figure 11. Valence phosphate cell 15927928 voltage and temperature profile during crush test.

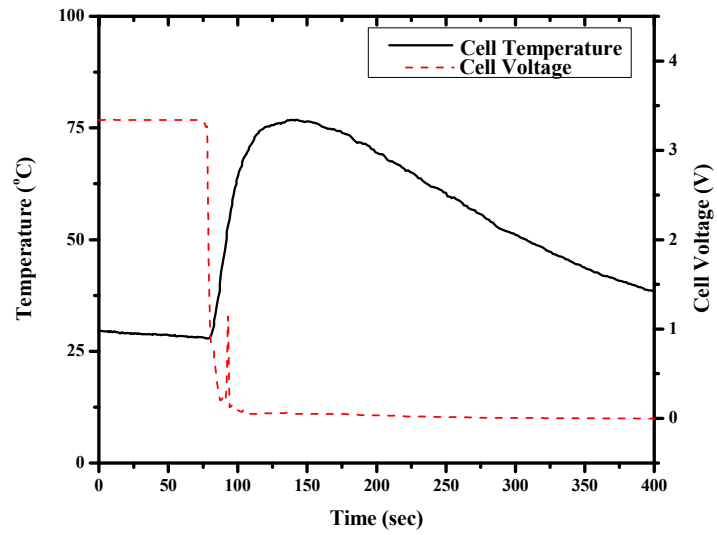


Figure 12. Valence phosphate cell 15929364 voltage and temperature profile during crush test.

The peak cell skin temperature measured for each of the cells during the crush testing is shown in Table 1. In comparison to the commercially available lithium cobalt oxide/mixed oxide 18650 cell types, the phosphate cells stayed substantially cooler during the thermal runaway with a peak skin temperature ranging from 77 °C to 111 °C. The peak skin temperature of the commercially available lithium mixed oxide 18650 cell and lithium cobalt oxide 18650 cell cells ranged from 260 °C to 297 °C, and 231 °C to 543 °C, for 3 cells tested each respectively.

These peak temperatures are significant when one considers the auto-ignition temperatures (445-465 °C) of organic solvents used in common Li⁺ electrolytes (see Table 2). In one instance, a commercially available lithium cobalt oxide 18650 cell (1012155) showed a peak skin temperature of 543 °C, indicating the possibility of this cell type to reach temperatures capable of causing auto-ignition of the organic solvents used in Li⁺ electrolytes. Additionally, the average skin temperatures for the commercially available lithium cobalt oxide/mixed oxide 18650 cells are above the temperature required to cause separator shutdown (as evidenced in the external heating experiments shown in the following section of this report). These facts have important implications for cells assembled in a pack because it would be feasible for a high quality commercially available lithium cobalt oxide/mixed oxide 18650 cells in thermal runaway to initiate thermal runaway in adjacent cells depending on the prevalent heat transfer characteristics and the possible occurrence of open flaming.

In contrast, the temperature of the phosphate cells did neither approach the thermal runaway temperature of the electrolyte, nor the temperature required for separator shutdown. Therefore, it is unlikely that the Valence phosphate cells suffering from an internal cell fault could initiate thermal runaway in adjacent cells even with proper heat transfer conditions.

Table 1. Summary of peak cell skin temperatures during crush testing

Cell ID	Peak Cell Skin Temperature (°C)	Flaming Combustion
Li(Co _{1/3} Ni _{1/3} Mn _{1/3})O ₂ 2007964	297	No
Li(Co _{1/3} Ni _{1/3} Mn _{1/3})O ₂ 2002828	260	No
Li(Co _{1/3} Ni _{1/3} Mn _{1/3})O ₂ 2006711	290	No
LiCoO ₂ 1008751	345	Yes
LiCoO ₂ 1008750	231	No ²
LiCoO ₂ 1008736	286	No
LiCoO ₂ 1012155	543	Yes
Phosphate 15930855	111	No
Phosphate 15927928	79	No
Phosphate 15929364	77	No

Table 2. Auto-ignition temperatures for common Li⁺ electrolytes³.

Organic Solvent	Common Abbreviation	Auto-Ignition Temperature
Propylene Carbonate	PC	455 °C
Ethylene Carbonate	EC	465 °C
Dimethyl Carbonate	DMC	445 °C
Diethyl Carbonate	DEC	445 °C

² No continuous flaming combustion but flame was observed when the cell vented.

³ Source: Material Safety Data Sheets

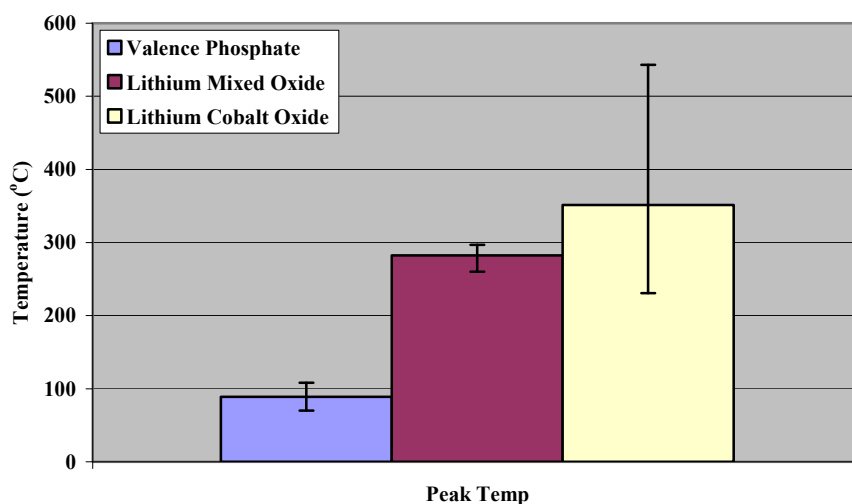


Figure 13. Summary of peak cell skin temperature during crush test. Error bars indicate one standard deviation from the mean.

Weight loss due to venting of gases and electrolyte from the cells during the crush tests is shown in Figure 14. Both of the commercially available lithium cobalt oxide/mixed oxide 18650 cell types lost substantially more mass, presumably due to decomposition of the cathode, combustion and/or evaporation of the electrolyte and ejection of other volatile materials from the cell. The slightly higher percentage of mass loss exhibited by the commercially available lithium cobalt oxide 18650 cells compared to the mixed oxide 18650 cells is due to the crimp releasing on one of the cells, resulting in the ejection of half of the cell windings. These findings are consistent with temperatures recorded for these cell types that were above the boiling point for the common Li^+ electrolyte solvents and the observation of flames on venting in some instances.

In contrast, the phosphate cells lost relatively little mass due to thermal events induced by crush testing. This finding is consistent with relative low cell temperatures during crush testing.

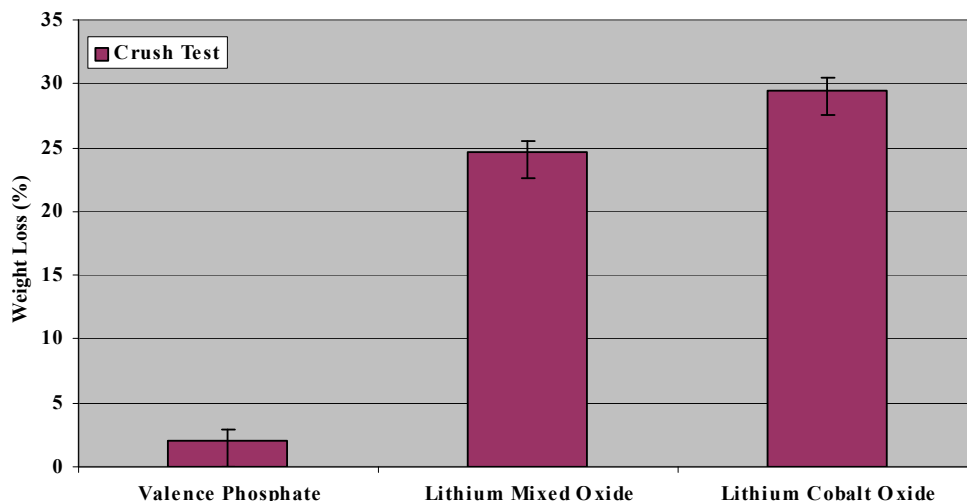


Figure 14. Average cell weight losses after crush testing. Error bars indicate range of weight loss.

Figure 15 through Figure 24 show the post-test X-ray images of the ten crush tested cells. The bottom X-ray image in each figure was taken by rotating the cells 90° about the cell center axis relative to the position where the top X-ray image was taken.

Figure 15 through Figure 17, and Figure 22 through Figure 24, show X-ray images of the commercially available lithium mixed oxide 18650 cells and phosphate cells, respectively. All six of these cells failed without flames. Examination of the X-ray images indicates the layers of the cell windings are still visible and presumably intact, save for the deformation caused by the crush test. Layers of the cell windings are observed and the cap assembly is still in place suggesting relatively benign venting events.

Figure 18 through Figure 21 show X-ray images for the commercially available lithium cobalt oxide 18650 cells that underwent crush testing. In contrast to the other two cell types, these cells all failed with observation of flames and two cells failed continuous flaming. Three of the cells show obvious perforation of the cap assembly most likely caused by escaping flames. The fourth cell (1008751) showed separation of the cap assembly from the cell can.

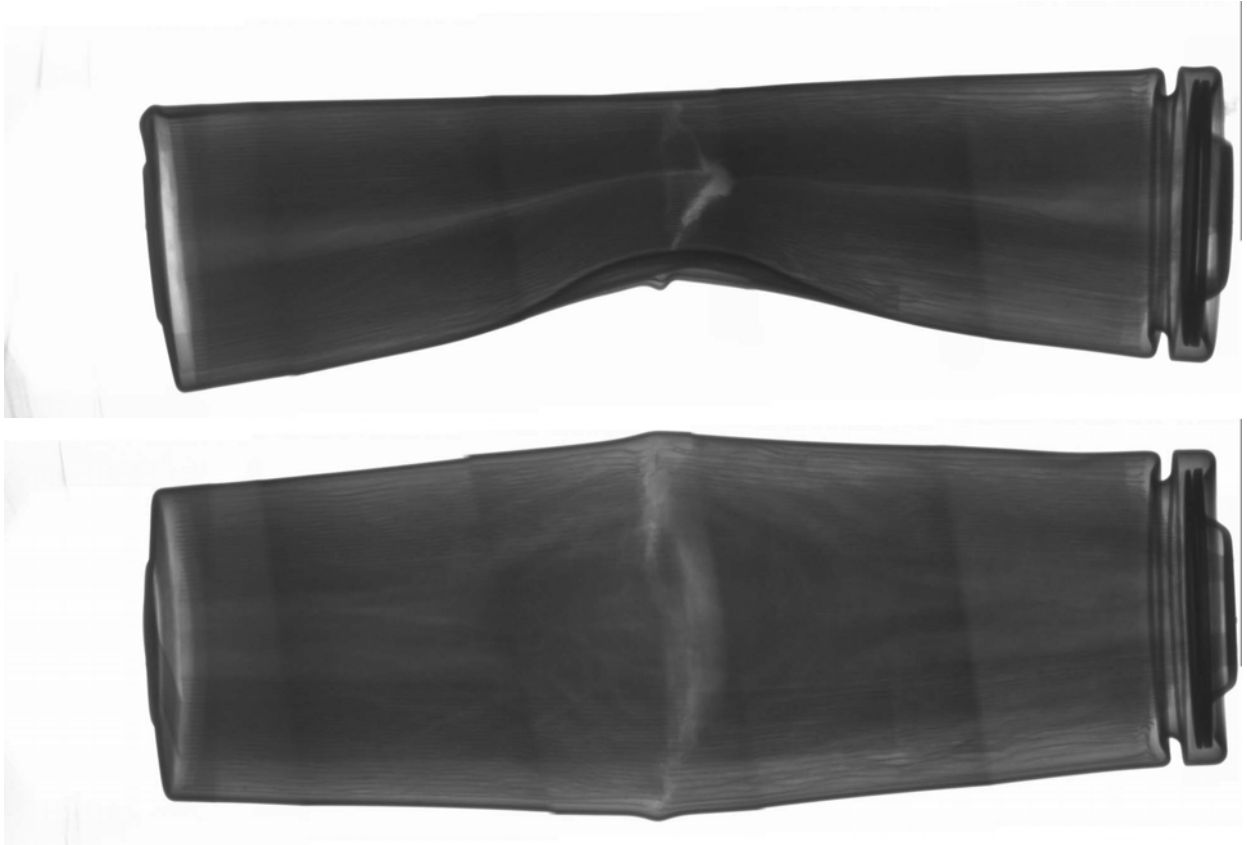


Figure 15. Post crush test X-ray image of $\text{Li}(\text{Co}_{1/3}\text{Ni}_{1/3}\text{Mn}_{1/3})\text{O}_2$ cell 2007964.

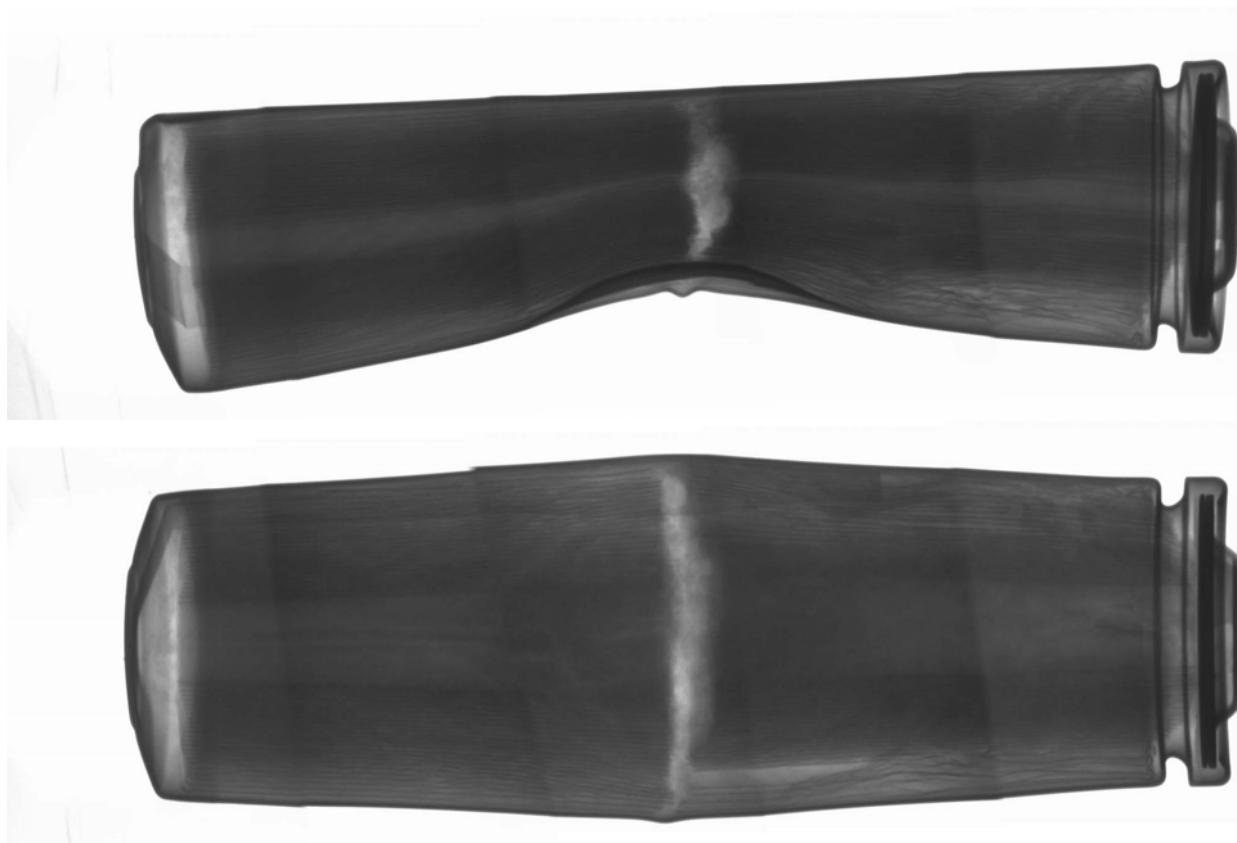


Figure 16. Post crush test X-ray image of $\text{Li}(\text{Co}_{1/3}\text{Ni}_{1/3}\text{Mn}_{1/3})\text{O}_2$ cell 2002828.

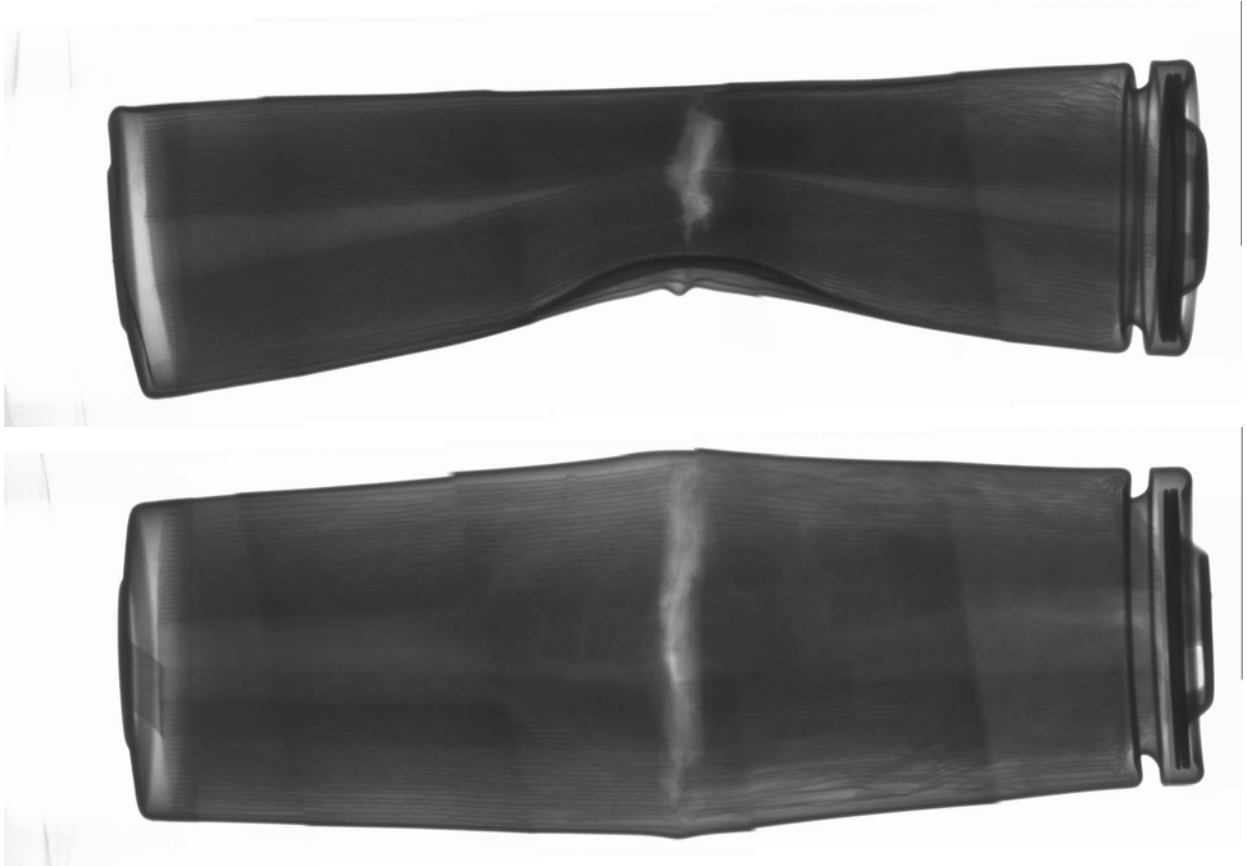


Figure 17. Post crush test X-ray image of $\text{Li}(\text{Co}_{1/3}\text{Ni}_{1/3}\text{Mn}_{1/3})\text{O}_2$ cell 2006711.

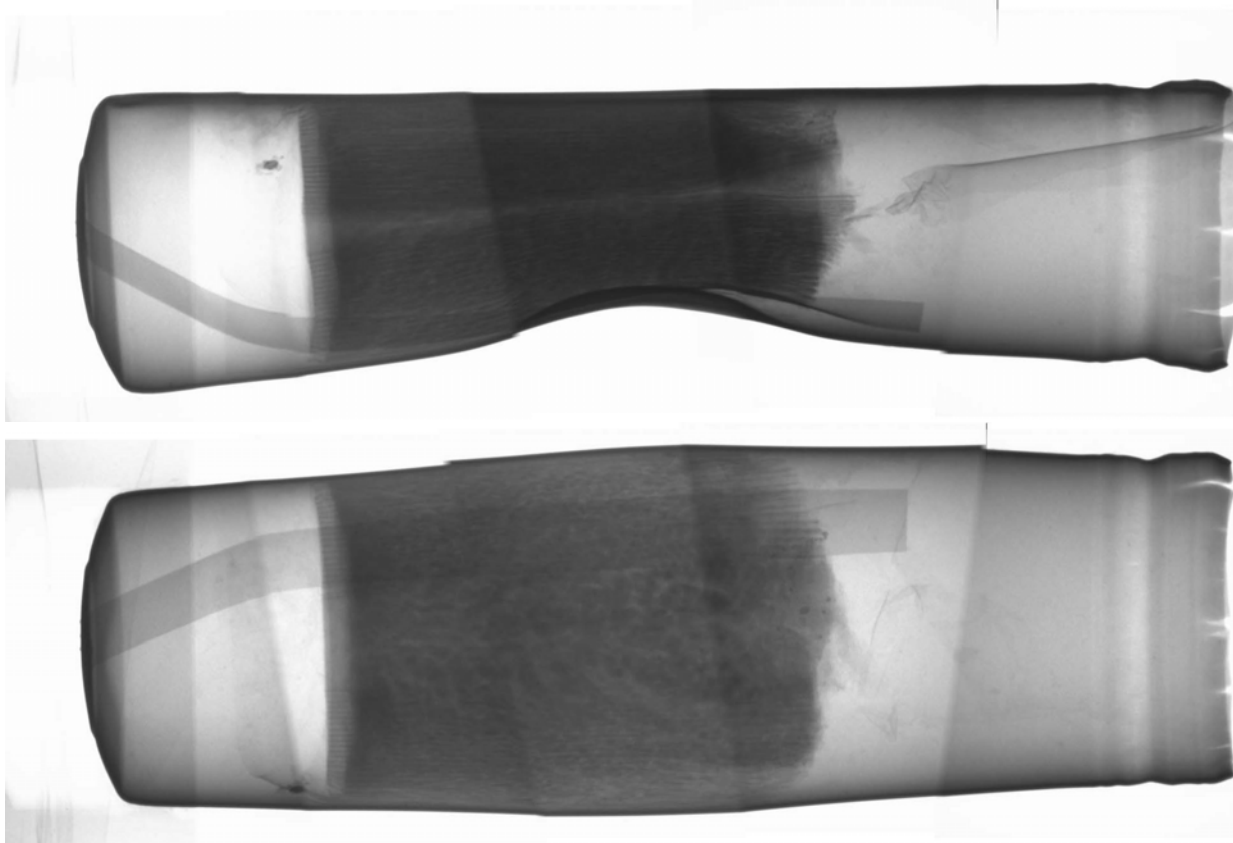


Figure 18. Post crush test X-ray image of LiCoO_2 cell 1008751.

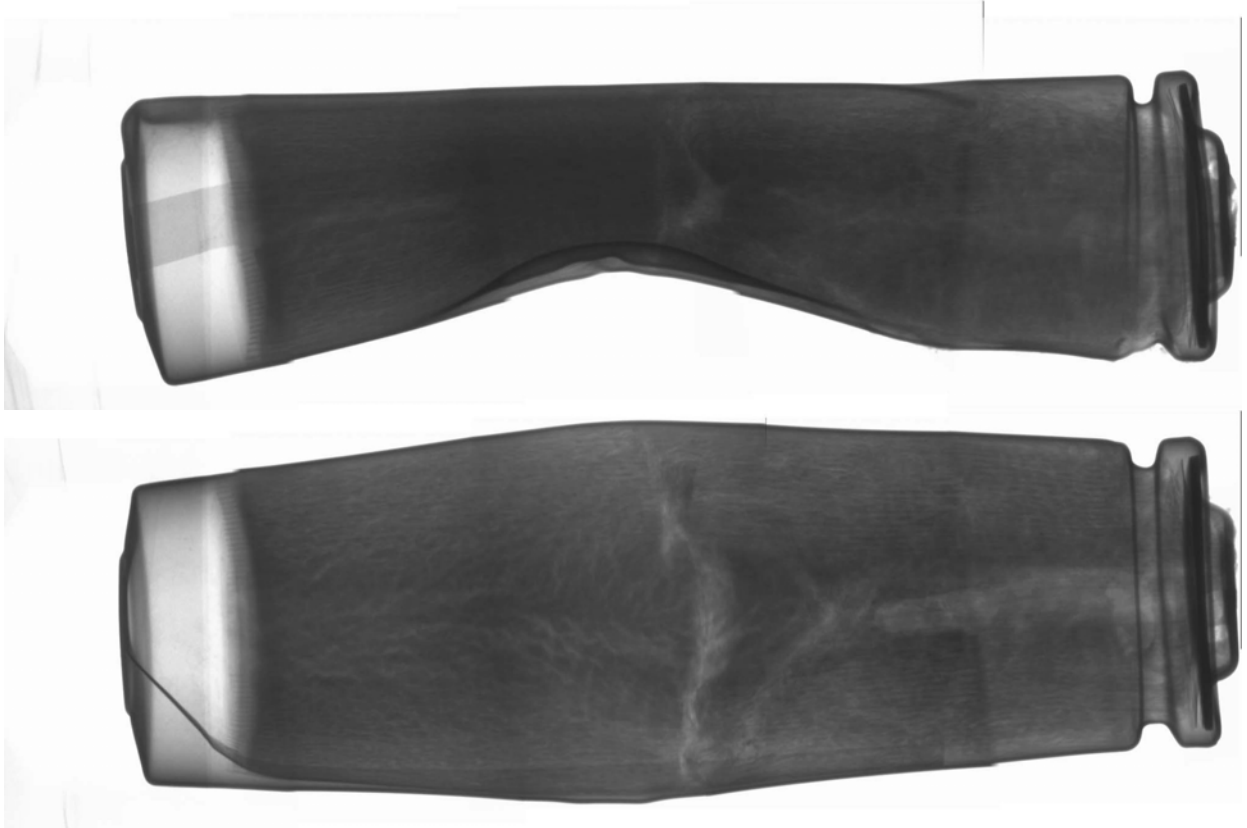


Figure 19. Post crush test X-ray image of LiCoO_2 cell 1008750.

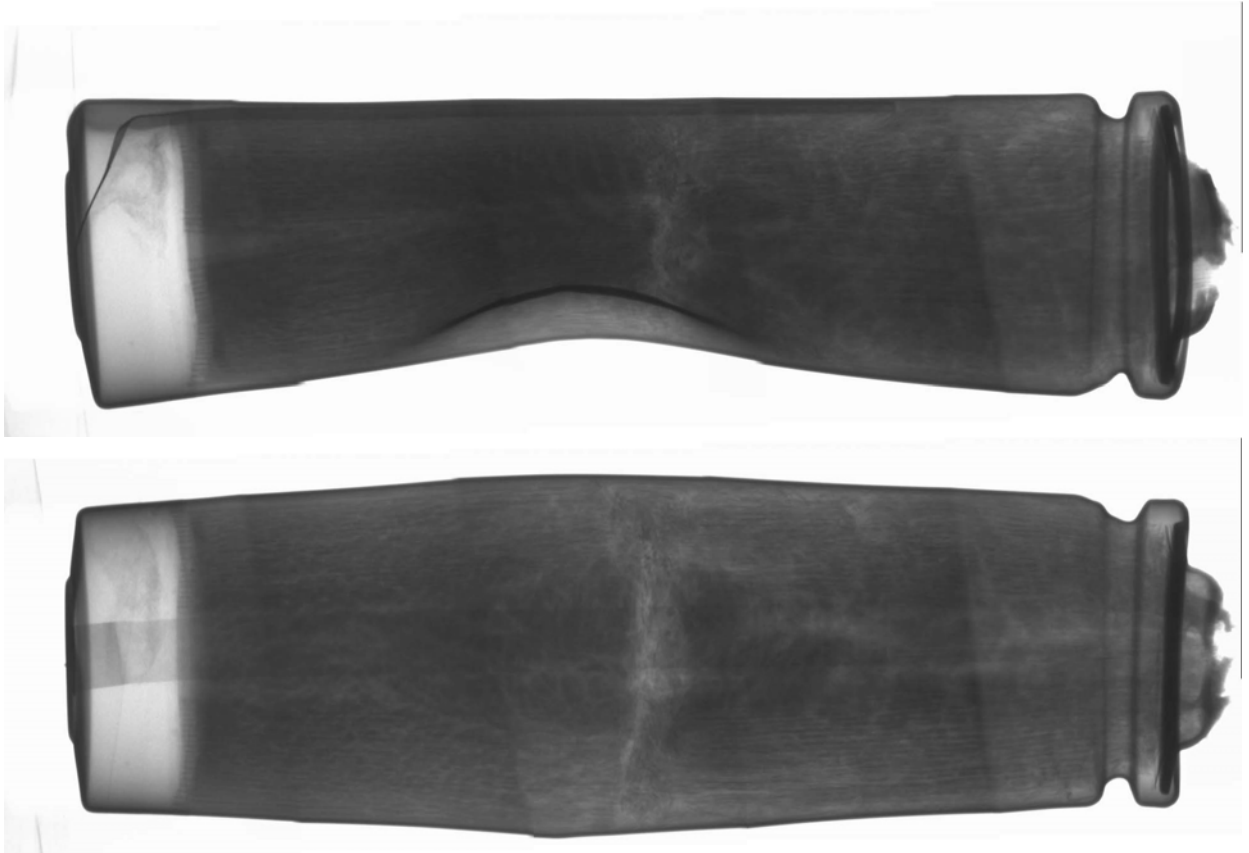


Figure 20. Post crush test X-ray image of LiCoO_2 cell 1008736.

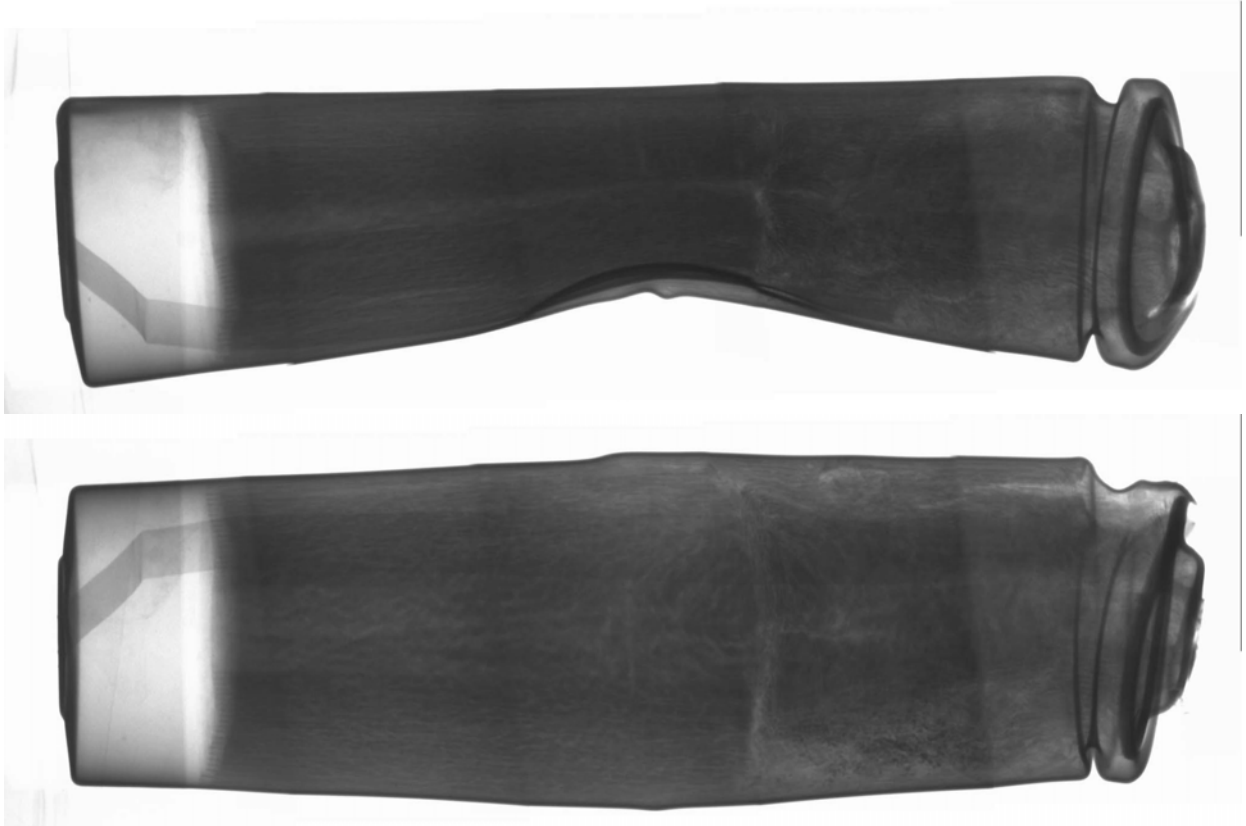


Figure 21. Post crush test X-ray image of LiCoO₂ cell 1012155.

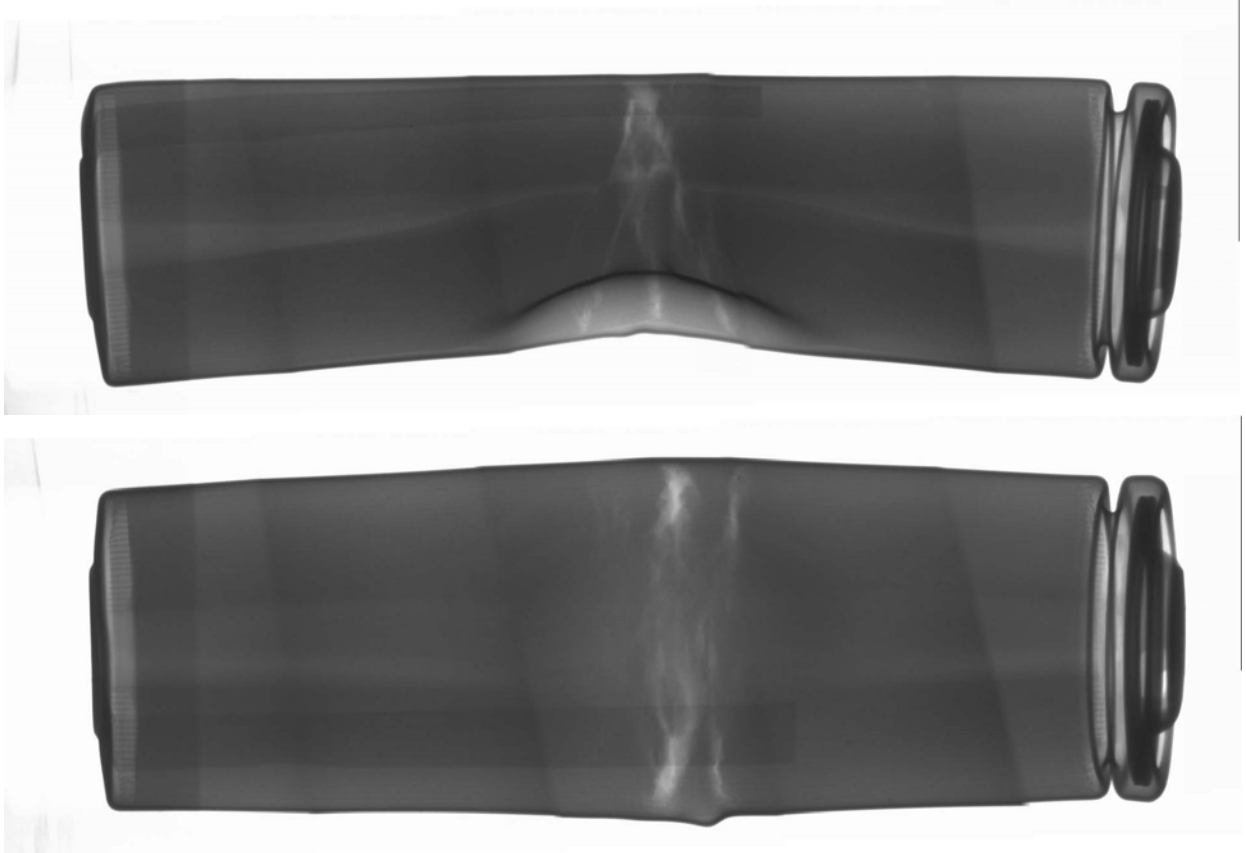


Figure 22. Post crush test X-ray image of phosphate cell 15930855.

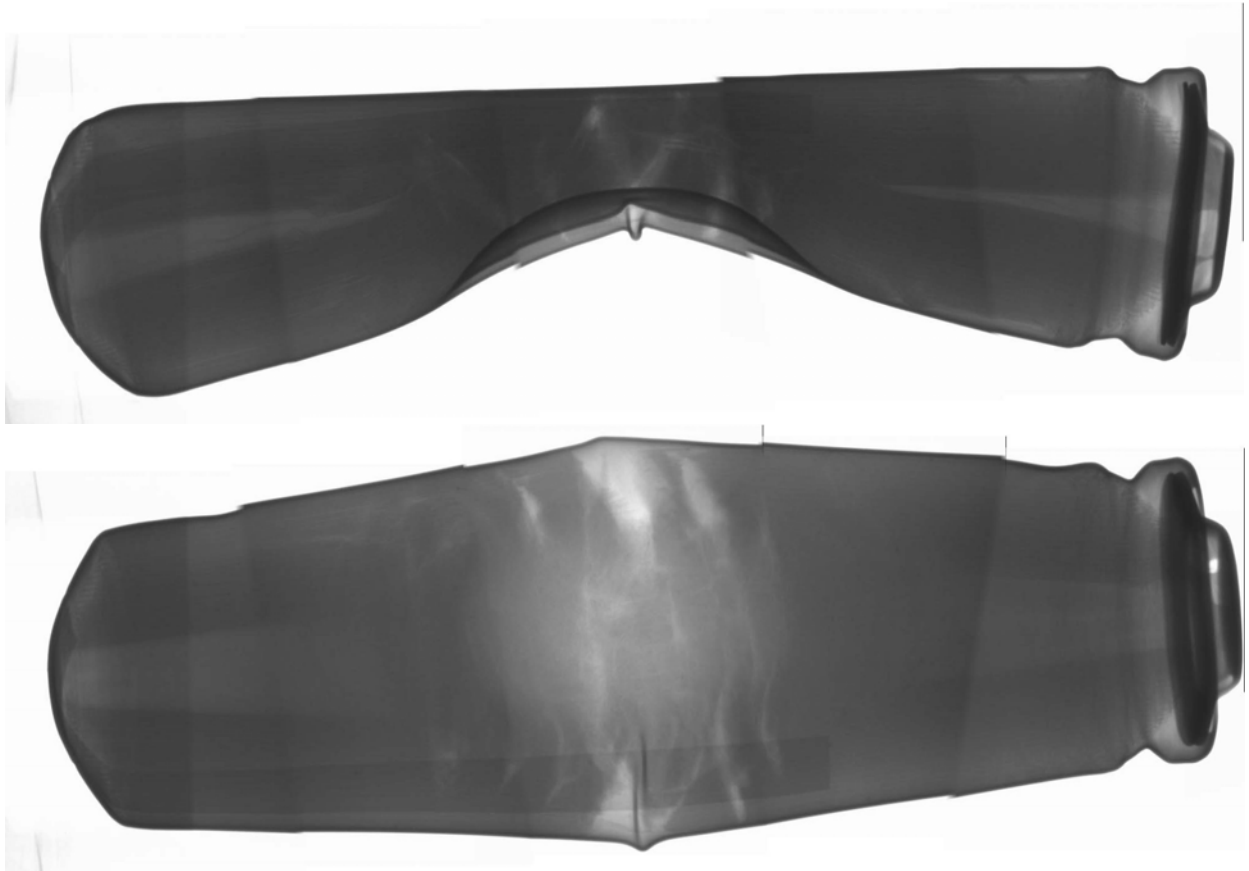


Figure 23. Post crush test X-ray image of phosphate cell 15927928.

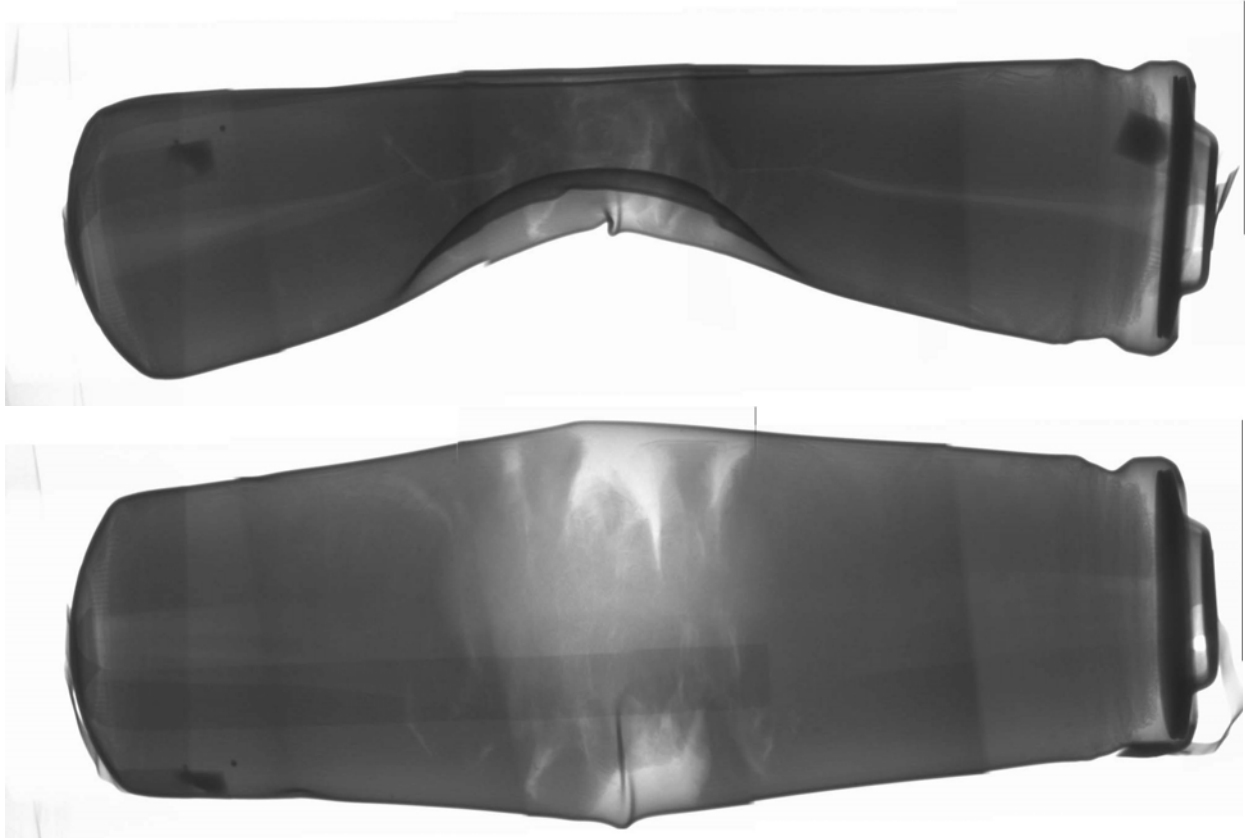


Figure 24. Post crush test X-ray image of phosphate cell 15929364.

Test Summary

Results from the crush tests are as follows:

- The phosphate cells tested failed benignly without flaming at temperatures below 112 °C making spread of thermal runaway from one cell with an internal fault to adjacent cells in a battery pack improbable.
- The commercially available lithium mixed oxide 18650 cells selected for these tests failed benignly without flaming, and reached temperatures that approach 300 °C. It would be possible for these cells to cause separator shutdown in adjacent cells in a battery and propagate thermal runaway through the pack.

- The commercially available lithium cobalt oxide 18650 cells selected for these tests failed energetically, with flames and reached temperatures as high as 543 °C. It would be possible for these cells to cause auto-ignition of electrolyte, separator shutdown in adjacent cells in a battery and propagate thermal runaway through the pack.

2. Heating Test

Test Purpose

Heat from an external source was applied to the various chemistry lithium-ion cells in order to determine the effect that differing cathode chemistry had on the initiation temperature for thermal runaway.

Test Setup

Cells were charged to 100% SOC per manufacturers' specifications. A small tube furnace was constructed from cast iron pipe wrapped with a 115 V AC heater tape, as shown in Figure 25, Figure 26, and Figure 27. The tube furnace was controlled with a high power variable resistor that was used to control the heating ramp rate (~ 15 °C/minute). A secondary aluminum cover was used to contain an insulation layer that reduced radiative losses from the tube furnace (Figure 25). The temperature of the furnace was monitored between the cast iron pipe and the heat tape by a J-type thermocouple (Figure 25). Steel bolts at the ends of the tube furnace were used to contain the cell and ensure that upon venting and thermal runaway the cell remained in the tube furnace (Figure 25). A small piece of cheese cloth was placed ~ 1 cm in front of the cell vent to catch material ejected from the cell.

Cells were instrumented with J-type thermocouples to measure the temperature of the cell skin near the center of the cell. Cell voltage was continuously monitored over the course of the experiment. Additionally, the ambient temperature and tube furnace temperature were recorded for the duration of the experiment. All experiments were videotaped to capture the cell response and possible venting behavior of the cell and allow for qualitative comparison across the cell types tested.

The tube furnace was turned off immediately after initiation of a thermal event as determined by the rapid decrease in cell voltage. The temperature and voltage measurements were continued

until the cell skin temperature dropped to below 50 °C. The cell skin temperature and cell voltage were reported as a function of time. The temperature at which the separator broke down (as determined by the initiation of cell voltage drop), the temperature at which thermal runaway initiated (indicated by a rapid increase in the temperature) and the peak temperature were reported.

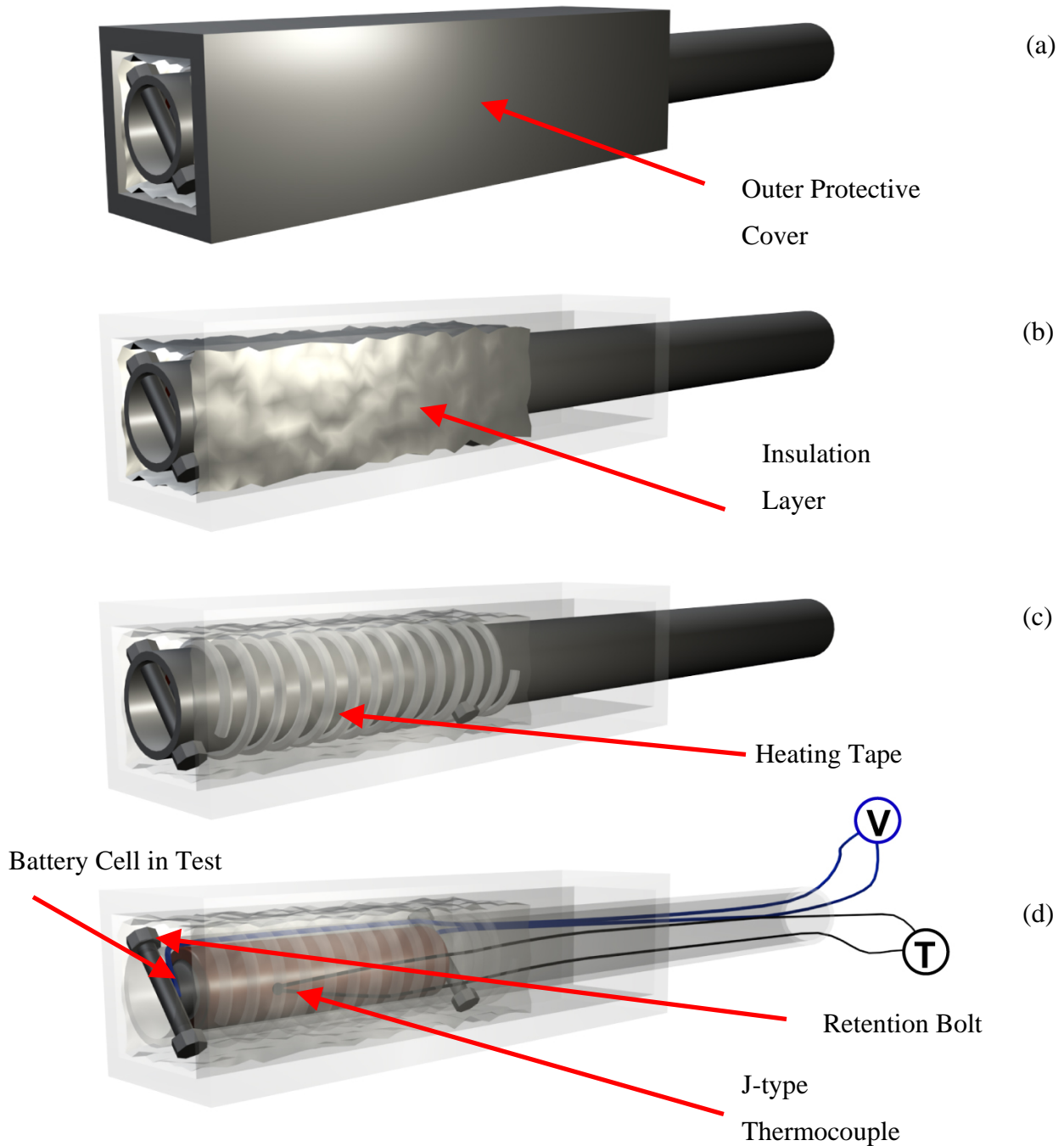


Figure 25. a) Schematic break down of heat test apparatus. b) Underneath the protective covering layer insulation was used to prevent radiative heat loss from the c) heat tape wrapped around the center heater tube. d) The temperature of the test apparatus was monitored with a J-type thermocouple located between the heating tape and the center heater tube. Bolts located near both ends of the cell prevent the cell from being ejected when the cell vented.



Figure 26. Photograph of heat test apparatus.



Figure 27. Photograph of heat test apparatus supported in laboratory press for testing.

Figure 28, Figure 29 and Figure 30 show the X-ray images of the three types of cells prior to testing. The X-ray images show that none of the cells employ a center tube to facilitate the venting process.



Figure 28. Exemplar commercial lithium mixed oxide cell pre-test X-ray.

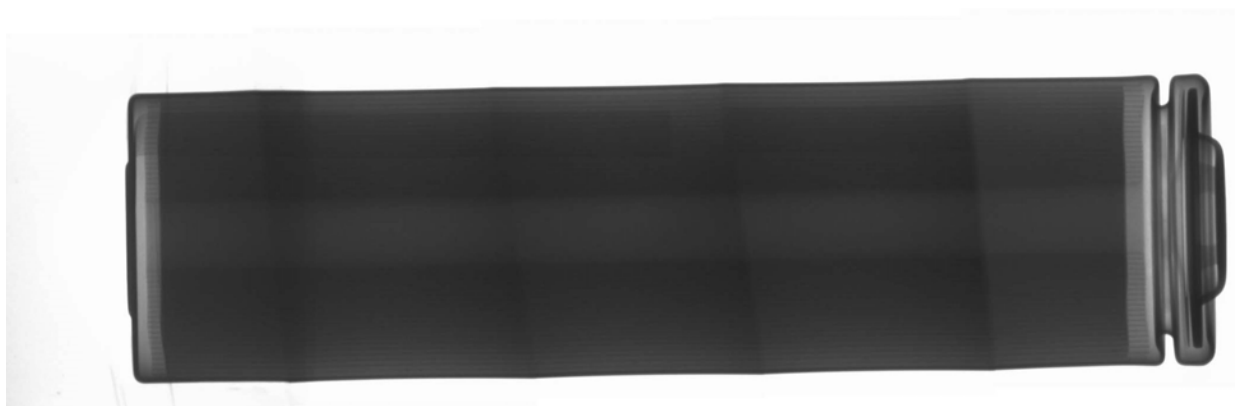


Figure 29. Exemplar commercial lithium cobalt oxide cell pre-test X-ray.

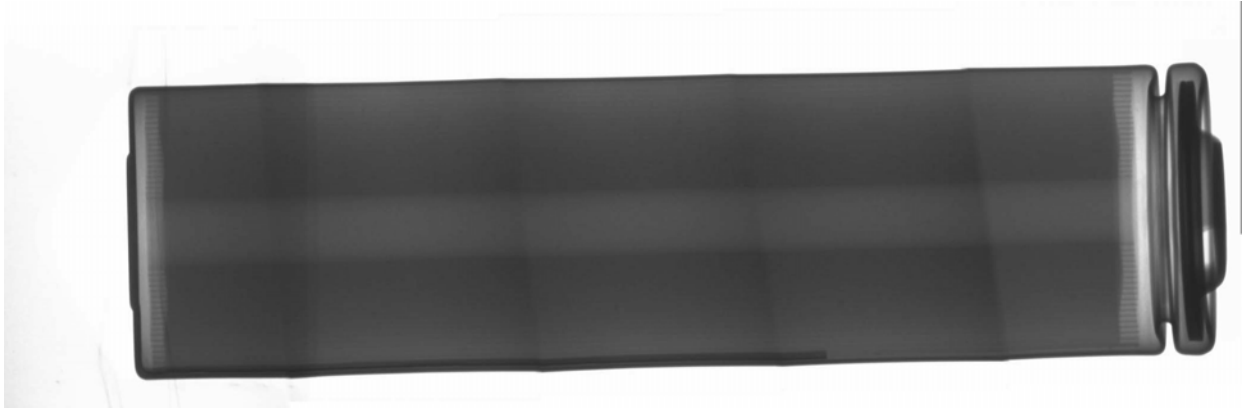


Figure 30. Exemplar Valence phosphate cell pre-test X-ray.

Test Results

Figure 31 through Figure 39 show the recorded voltage and temperature profiles of the nine cells tested during the external heating tests. When subjected to external heating, the cells exhibited characteristic behaviors that were assigned to physical or chemical changes within the cell:

1. A rapid decrease in cell voltage that was attributed to the melting of the separator;
2. A rapid increase in cell skin temperature, exceeding the external heater temperature, which is indicative of the initiation of exothermic chemical reactions that are associated with thermal runaway.

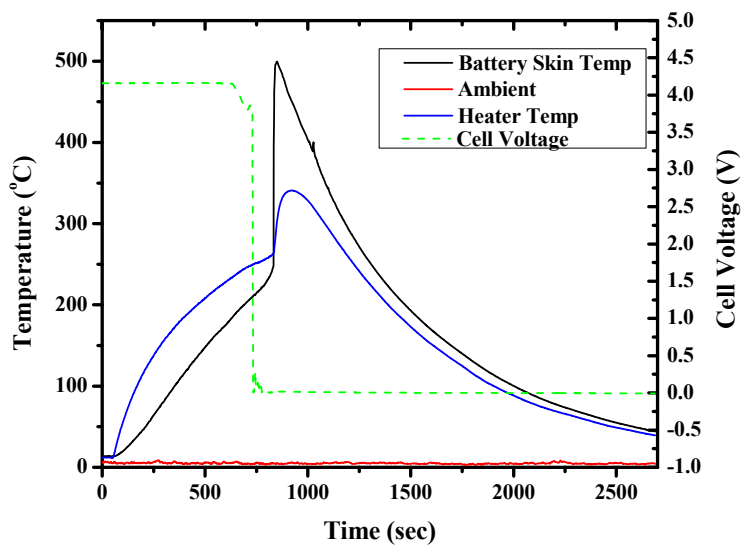


Figure 31. $\text{Li}(\text{Co}_{1/3}\text{Ni}_{1/3}\text{Mn}_{1/3})\text{O}_2$ cell 2007149 voltage and temperature profile during heat test.

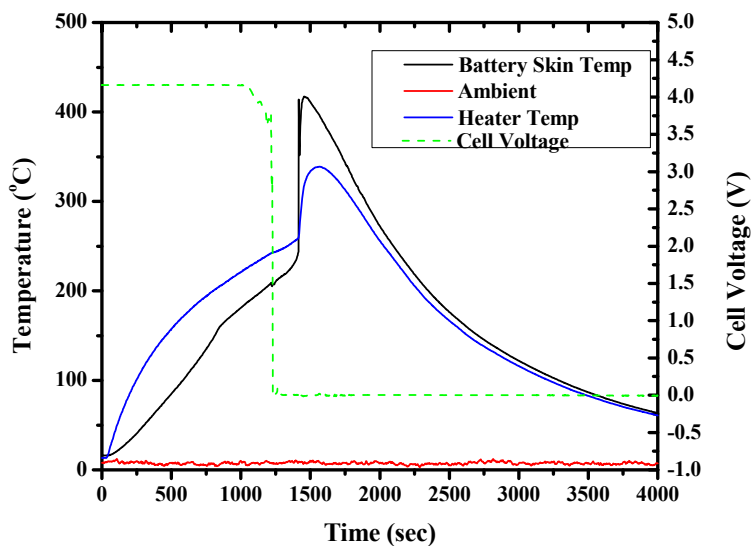


Figure 32. $\text{Li}(\text{Co}_{1/3}\text{Ni}_{1/3}\text{Mn}_{1/3})\text{O}_2$ cell 2007023 voltage and temperature profile during heat test.

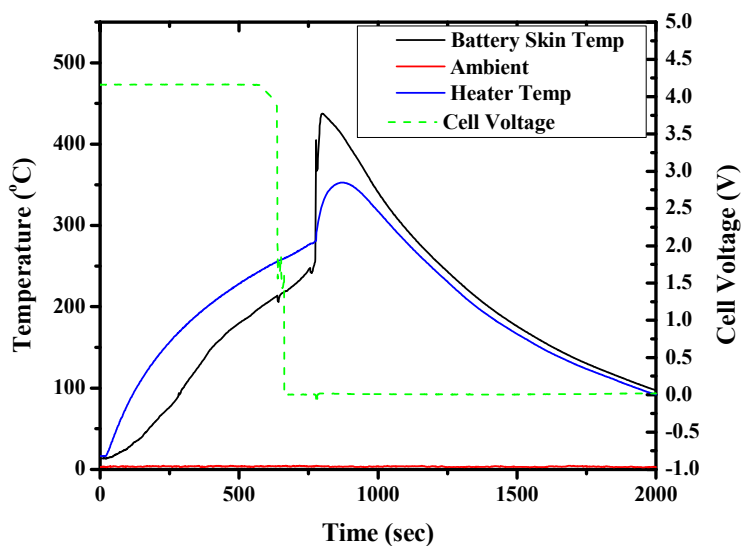


Figure 33. $\text{Li}(\text{Co}_{1/3}\text{Ni}_{1/3}\text{Mn}_{1/3})\text{O}_2$ cell 2001015 voltage and temperature profile.

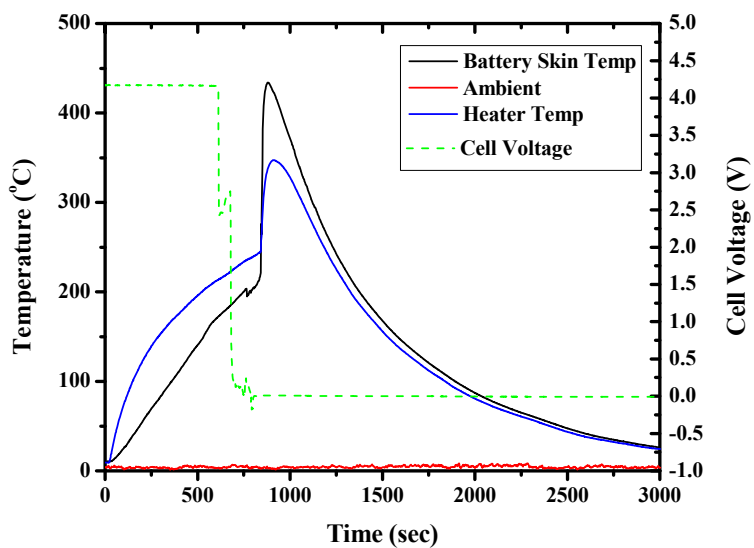


Figure 34. LiCoO_2 cell 1012133 voltage and temperature profile during heat test.

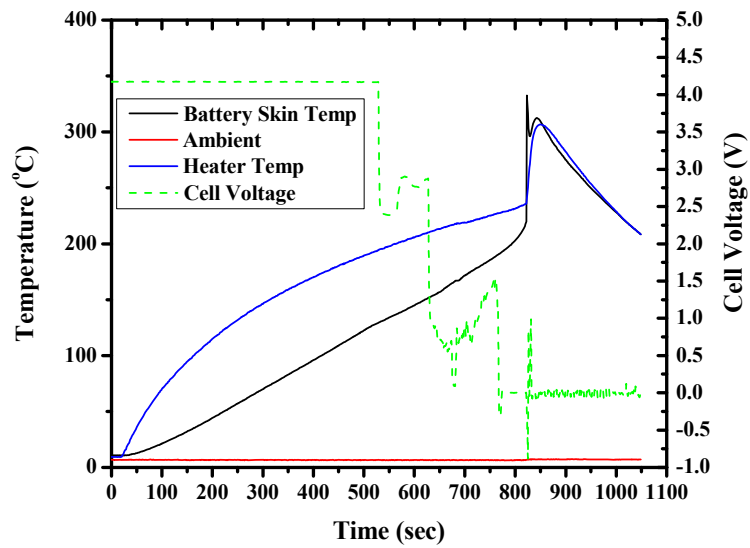


Figure 35. LiCoO₂ cell 1008815 voltage and temperature profile during heat test.

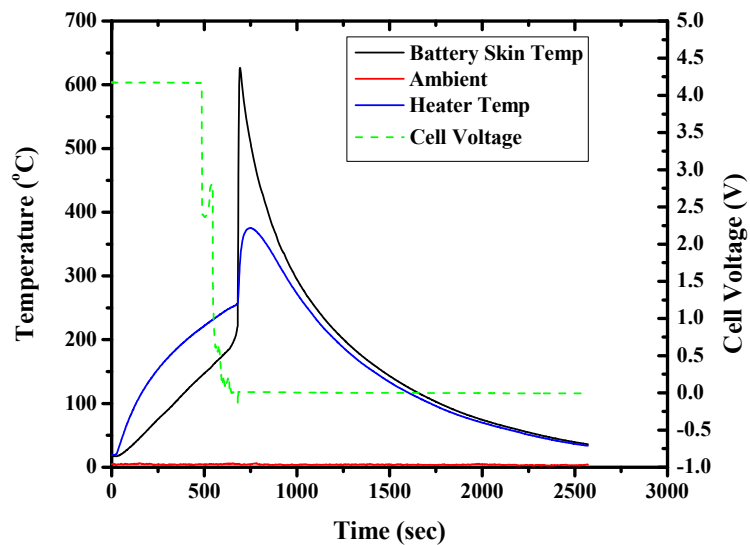


Figure 36. LiCoO₂ cell 1012144 voltage and temperature profile during heat test.

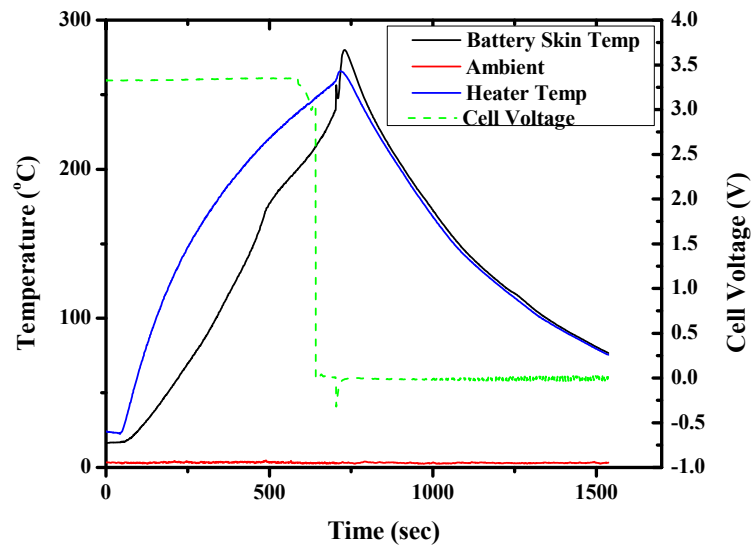


Figure 37. Phosphate cell 15930325 voltage and temperature profile during heat test.

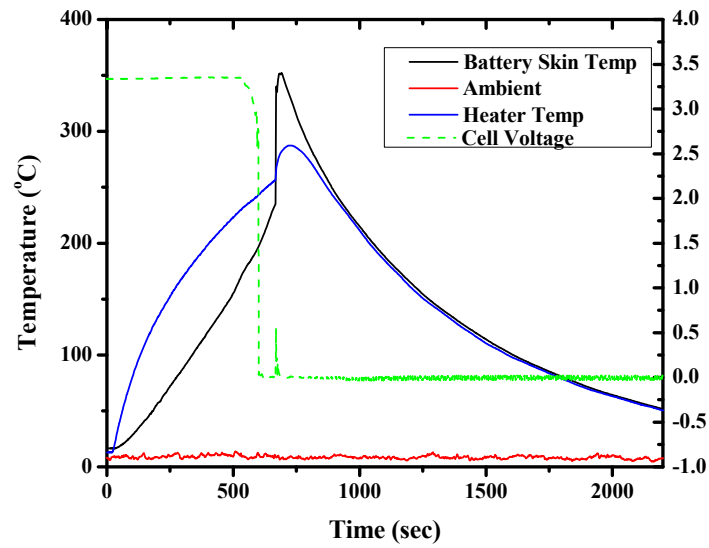


Figure 38. Phosphate cell 15929411 voltage and temperature profile during heat test.

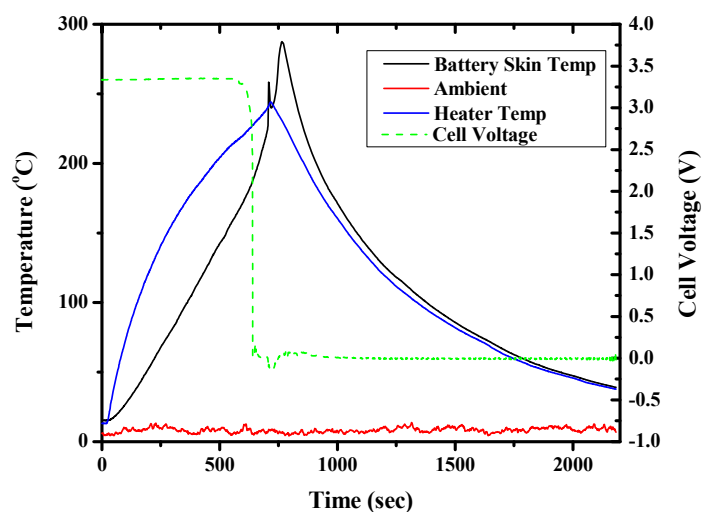


Figure 39. Phosphate cell 15927964 voltage and temperature profile during heat test.

Table 3 and Figure 40 summarize the three critical cell skin temperatures during the heating test:

- Temperature at separator shutdown;
- Temperature at the initiation of thermal runaway;
- Peak cell skin temperature during the test;

Separator Shutdown Temperature

Similar separator shutdown temperatures for the phosphate and commercially available lithium cobalt oxide 18650 cells (183 °C and 190 °C respectively) suggest similar separator chemistry and similar separator thickness. In comparison, at 150 °C, the separator shutdown temperature of the commercially available lithium mixed oxide 18650 cells was substantially lower. This

finding suggests that the chemistry and/or thickness of the commercially available lithium mixed oxide 18650 cells differ from the two former cell types.

Thermal Runaway Initiation Temperature

The initiation temperature of thermal runaway, defined as the sudden increase in the temperature of cell, is essentially equal for all of the cells. The average value for the commercially available lithium mixed oxide 18650 cells tested is slightly lower and may be the result of earlier initiation of separator shutdown. Similarity in thermal runaway initiation temperature across the three cell types tested is consistent with the theory that thermal runaway results from exothermic breakdown of the secondary solid-electrolyte interface (SEI) layer at the anode⁴. It is assumed that the anode material for the three cell types is graphite and that similar secondary SEI layers formed under the given experimental conditions.

Peak Skin Temperature

At 306 °C, the average peak temperature for the phosphate cells was the lowest. Average peak temperature for the commercially available lithium cobalt oxide/mixed oxide 18650 cells were similar (461 and 452 °C, respectively) and substantially higher. It is important to note that the range of peak temperatures for the commercially available lithium 18650 cells tested showed temperatures up to 498 °C for the mixed oxide type and up to 622 °C for cobalt oxide cells.

⁴ H. Yang, S. Amiruddin, H. J. Bang, Y-K. Sun, J. Prakash, *J. Ind. Eng. Chem.* (12)1, 12-38 (2006)

Table 3. Summary of cell skin temperature during heat test.

Cell ID	Separator Shutdown Temperature (°C)	Thermal Runaway Initiation Temperature (°C)	Peak Temperature (°C)	Ignition of Cheese Cloth
Li(Co _{1/3} Ni _{1/3} Mn _{1/3})O ₂ 2007149	183	251	498	Yes
Li(Co _{1/3} Ni _{1/3} Mn _{1/3})O ₂ 2007023	189	243	418	Yes
Li(Co _{1/3} Ni _{1/3} Mn _{1/3})O ₂ 2001015	197	254	439	Yes
LiCoO ₂ 1012133	177	223	433	No
LiCoO ₂ 1008815	130	222	330	No
LiCoO ₂ 1012144	143	225	622	No
Phosphate- 15930325	202	242	281	No
Phosphate- 15929411	184	236	351	N/A ⁵
Phosphate- 15927964	163	227	286	No

⁵ Cheese cloth fell off before cell vent.

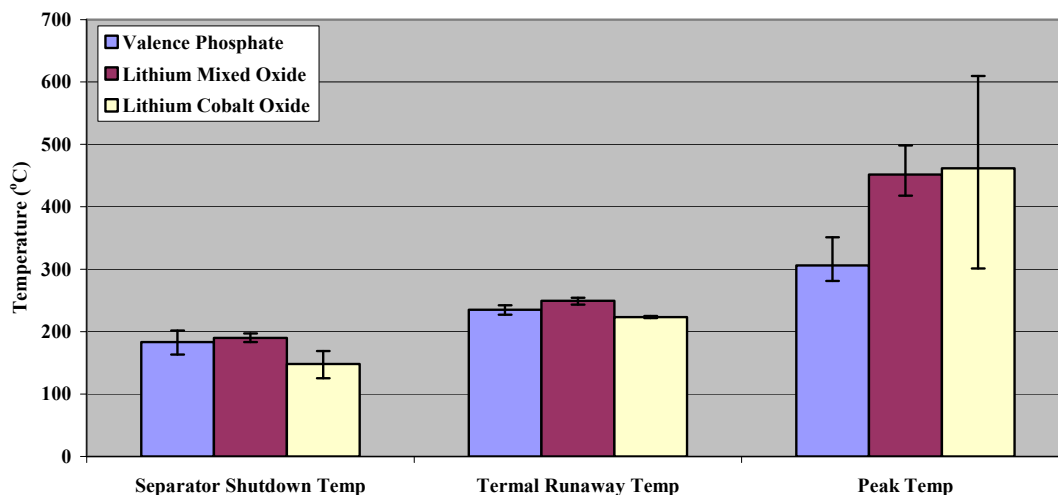


Figure 40. Summary of cell skin temperature during heating test. Error bars indicate the range of values measured.

X-ray Images of Cells After External Heating Tests

Lithium Mixed Oxide 18650 Cells

Figure 41, Figure 42 and Figure 43 are X-ray images of the three commercially available lithium mixed oxide 18650 cells after the external heating tests. The cells shown in Figure 41 and Figure 42 remained largely intact and show the cell windings and cap assembly in place. This suggests the vent operated properly in both cells. There is some bulging present in the cell shown in Figure 42 suggesting a higher pressure than that seen in the cell of Figure 41. The images also suggest some displacement of the cell windings occurred as a result of the venting force.

The cell depicted in Figure 43 shows a relatively large displacement of the cell windings toward the vent and an absence of the cap assembly. These conditions are most likely the result of vent

failure due to clogging and cap assembly crimp seal failure due to the excessive pressure within the cell.



Figure 41. Post heating test X-ray image of $\text{Li}(\text{Co}_{1/3}\text{Ni}_{1/3}\text{Mn}_{1/3})\text{O}_2$ cell 2007149.

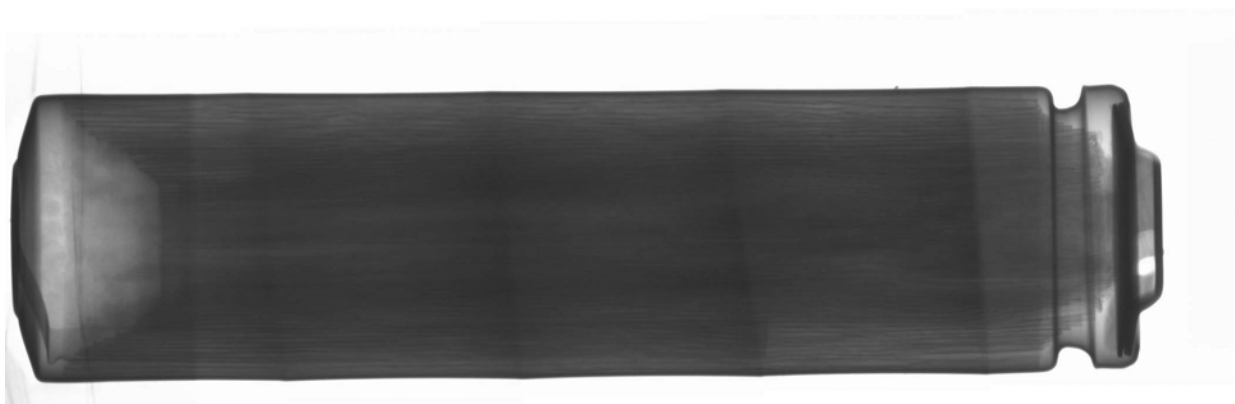


Figure 42. Post heating test X-ray image of $\text{Li}(\text{Co}_{1/3}\text{Ni}_{1/3}\text{Mn}_{1/3})\text{O}_2$ cell 2007023.



Figure 43. Post heating test X-ray image of $\text{Li}(\text{Co}_{1/3}\text{Ni}_{1/3}\text{Mn}_{1/3})\text{O}_2$ cell 2001015.

Lithium Cobalt Oxide 18650 cells

The failures associated with external heating of the commercially available lithium cobalt oxide 18650 cells tested appeared to be more energetic than those for the mixed oxide cells and resulted in the separation of the cap assembly from the cell in all three tests. In one cell, shown in Figure 44, the crimp assembly was torn off and the cell windings were completely ejected. Vent failure coupled with higher internal pressure is the likely cause of the observed failures and is consistent with higher peak skin temperatures.

Close examination of the X-ray images shown in Figure 45 and Figure 46 and comparison to the images for the mixed oxide cells shown above suggest that the temperatures inside the cell were sufficient to melt some of the material inside the can. This is evidenced by what appears to be nodules of aluminum (little black dots) at the edge of the electrodes. In contrast, the images for the mixed oxide cells do not exhibit these nodular features.

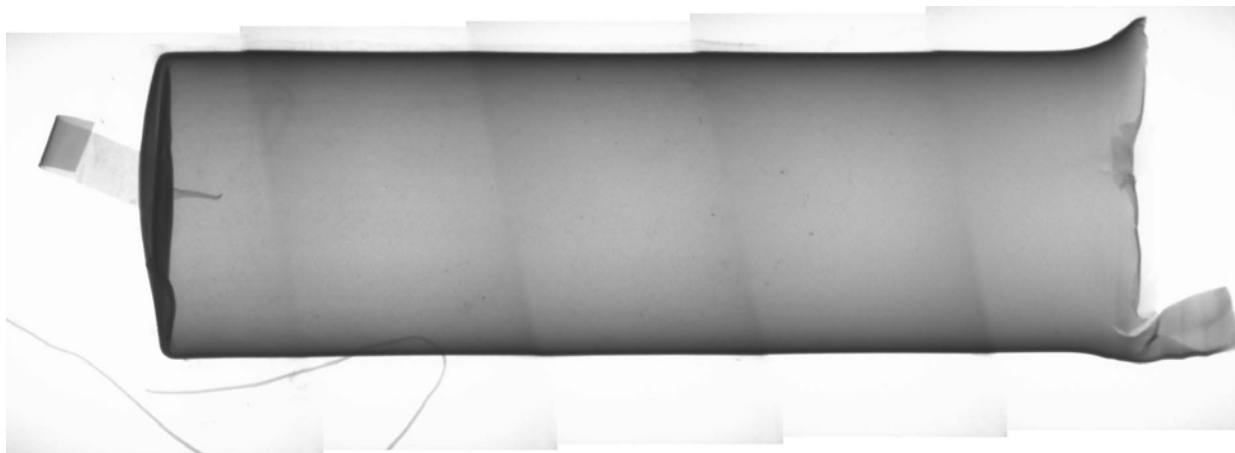


Figure 44. Post heating test X-ray image of LiCoO₂ cell 1012133.



Figure 45. Post heating test X-ray image of LiCoO₂ cell 1008815.



Figure 46. Post heating test X-ray image of LiCoO₂ cell 1012144.

Phosphate Cells

The severity of the failures associated with external heating of the phosphate cells were similar to those seen in the commercially available lithium cobalt oxide 18650 cells in that they also uniformly resulted in separation of the cap assembly from the cell. There is also evidence that a substantial portion of the cell windings from the cells shown in Figure 47 and Figure 49 were ejected from the cells.



Figure 47. Post heating test X-ray image of Valence phosphate cell 15930325.

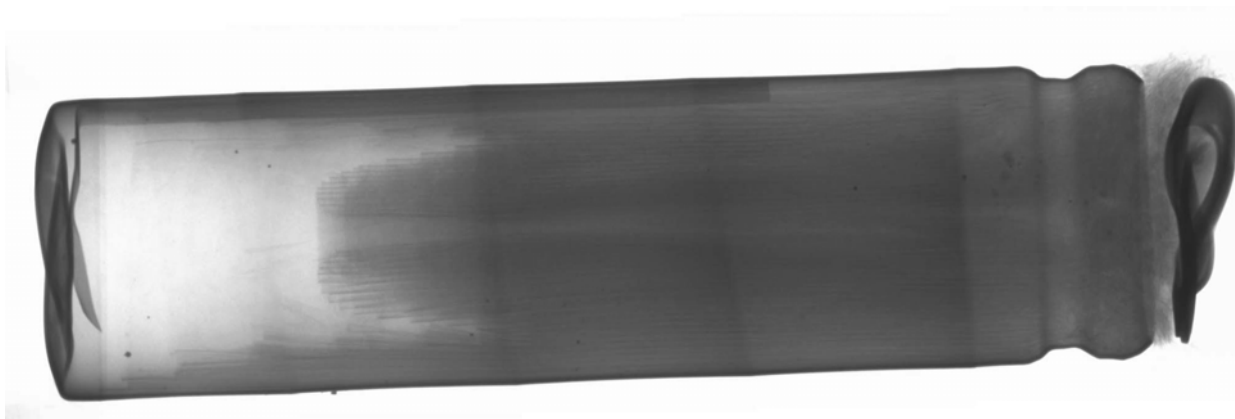


Figure 48. Post heating test X-ray image of Valence phosphate cell 15929411.

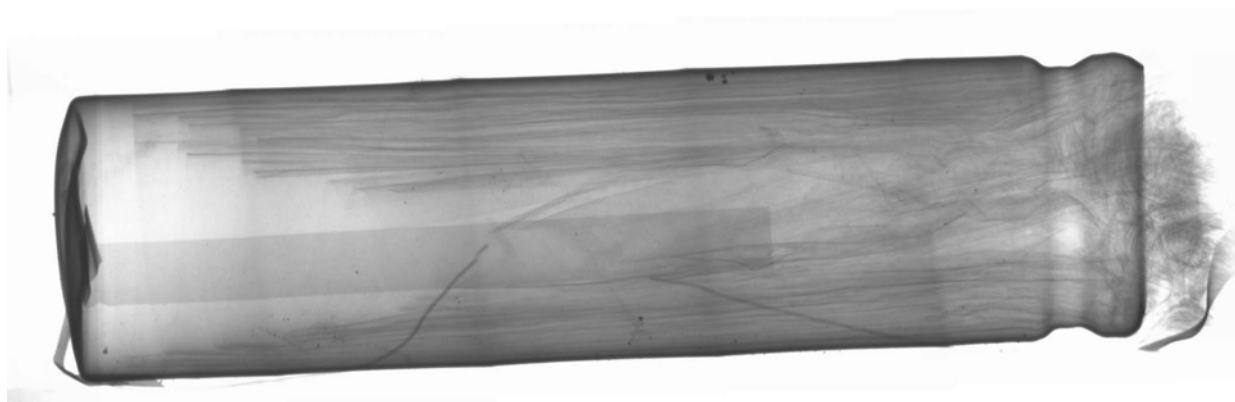


Figure 49. Post heating test X-ray image of Valence phosphate cell 15927964.

Test Summary

The results of the external heating test indicate:

- The temperature at separator shutdown was similar for all of the cells tested. The commercially available lithium mixed oxide 18650 cells tested showed breakdown at slightly lower temperature relative to the other two cell types suggesting a difference in separator chemistry or morphology.

- The temperature at which thermal runaway initiated was similar for all of the cells tested suggesting a common initiation mechanism. This mechanism is most likely a result of the exothermic chemical reactions that occur during the breakdown of the secondary SEI layer at the anode.
- Peak skin temperature was substantially higher for the commercially available lithium cobalt oxide/mixed oxide 18650 cells tested relative to the phosphate cells tested and was above the auto-ignition temperature for common Li^+ electrolyte solvents.

3. Accelerating Rate Calorimetry

Test Purpose

The goal of this testing was to determine the rate of temperature increase for selected 18650 cells made with various cathode chemistries. Exponent performed a series of tests at an external laboratory to measure fundamental thermal runaway parameters using accelerating rate calorimetry (ARC). ARC is a test method used to characterize exothermic reactions of a material. ARC data is used to evaluate a material's reactivity/instability under elevated temperature conditions and assess its potential hazards. ARC is conducted under adiabatic conditions (no heat flow occurs out of the system) in order to accurately measure the self-heating onset temperature, self-heating temperature rate, and pressure development.

Methods

Accelerating rate calorimeters are designed to maintain adiabatic conditions as exothermic self-heating reactions occur. The temperature was increased rapidly to the pre-selected start temperature of 50 °C then underwent a "Heat-Wait-Search" sequence where the temperature was raised 5 °C and held for a wait time of 20 minutes to determine if an exothermic, self-heating reaction occurred. If a self-heating reaction occurred that exceeded a predefined self-heating rate threshold of 0.02 °C/min, then the self-heating was allowed to occur and no further heat was supplied to the system externally. If, however, the self-heating rate threshold was not exceeded the sequence was repeated with an increase in temperature. The onset temperature at which self-heating occurred was recorded, and the self-heating rate, the peak temperature, and temperature at maximum rate were determined.

ARC can be conducted under both "closed" and "open" conditions referring to a sealed bomb or a bomb open to atmospheric conditions. In the "closed" condition the pressure evolution is measured. In some cases, the cell voltage potential can be monitored during testing.

Cells were charged according the manufacturers specified charge-discharge parameters and underwent one and a half cycles leaving them in the fully charged state at the beginning of the ARC test.

One cell of each cell type (Valence phosphate, commercially available lithium cobalt oxide and mixed oxide 18650 cells) was tested in the open ARC configuration and one cell each in the closed configuration. Time-temperature plots, time-pressure plots, and time-voltage plots are presented to determine specified parameters involved in exothermic self-heating breakdown of different Li-ion cell chemistries.

Temperature-time curves were measured during “seek and hold” increases in temperature during both open and closed ARC testing. During closed testing the voltage-time profiles were not measured because the ARC is not equipped for such measurements due to the sealed nature of the test apparatus. During open condition testing, however, the cell voltage potential was measured. When subjected to slow “seek and hold” ARC testing, all the tested cells exhibited similar behavior: Thermal runaway was detected at moderately low temperatures and continued until complete exothermic self-heating occurred.

Results

Temperature-time curves for the three Li-ion chemistry cells tested in both, the open and closed configurations are shown in Figure 50 to Figure 55. An initial rapid temperature increase from ambient temperature to 50 °C was observed followed by incremental 5 C increases in temperature until self-heating occurred. Temperature time curves indicated that a rapid increase in self-heating temperature occurred after a period of time. The rapid increase in temperature was characteristic of energetic thermal decomposition. All tests show energetic thermal decomposition with exception of the Valence phosphate closed test, which exhibited a gradual increase in self-heating, but no energetic thermal decomposition, as shown in Figure 53. Additionally, time-pressure curves demonstrated the energetic thermal decomposition of commercially available lithium cobalt oxide and mixed oxide 18650 cells tested, as shown in Figure 54 and Figure 55. As previously noted, the Valence phosphate cell did not undergo

energetic thermal decomposition, as noted also by the lack of a rapid increase in pressure associated with energetic thermal, as shown in Figure 53. In all cases, the self-heating onset temperature was shown to occur between 80 °C and 90 °C. A summary of the self-heating onset temperatures is provided in Table 4. The peak temperatures achieved are also apparent in Figure 50 to Figure 55. The peak temperatures achieved were between 245 °C and 550 °C. A summary of the peak adiabatic temperatures is shown in Table 4.

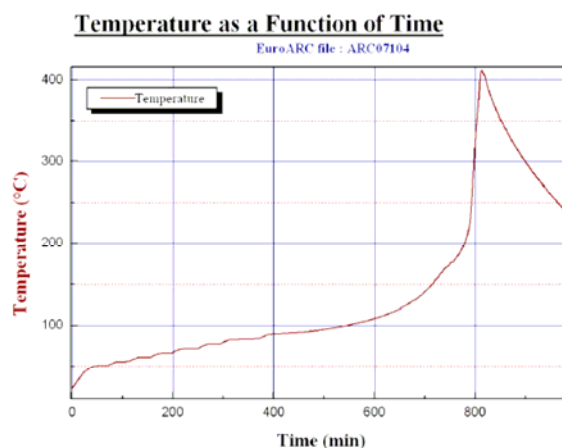


Figure 50. Temperature-time profiles of Valence phosphate 18650 cell tested in the open ARC configuration.

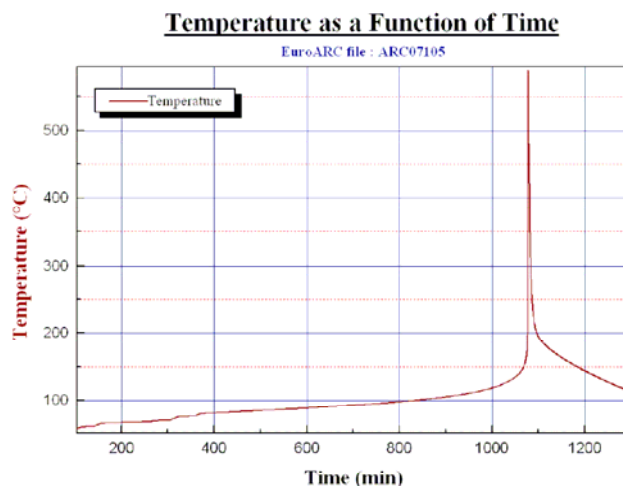


Figure 51. Temperature-time profiles of a commercially available lithium cobalt oxide 18650 cell tested in the open ARC configuration.

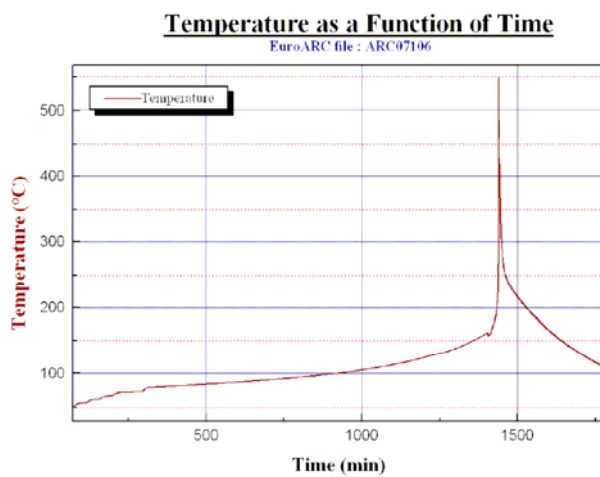


Figure 52. Temperature-time profiles of a commercially available lithium mixed oxide 18650 cell tested in the open ARC configuration.

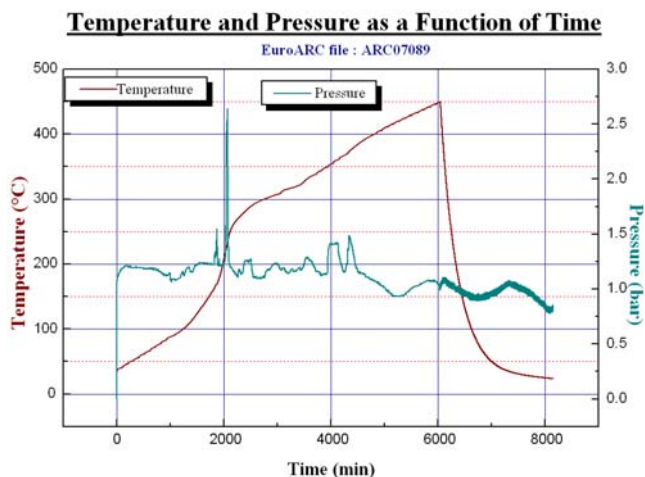


Figure 53. Temperature-time and temperature-pressure profiles of Valence phosphate 18650 cell tested in the closed ARC configuration.

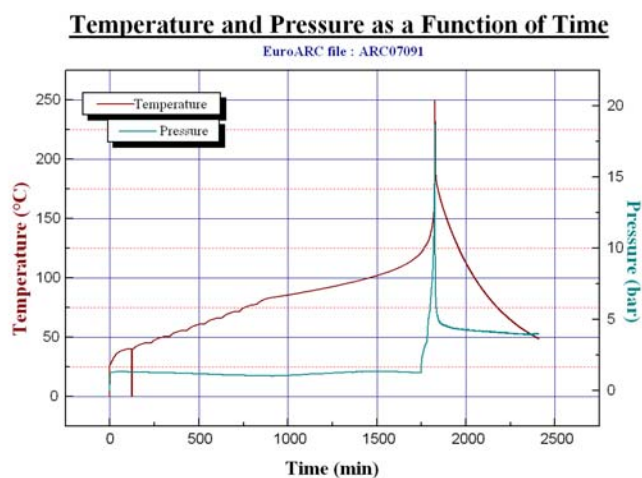


Figure 54. Temperature-time and temperature-pressure profiles of a commercially available lithium cobalt oxide 18650 cell tested in the closed ARC configuration.

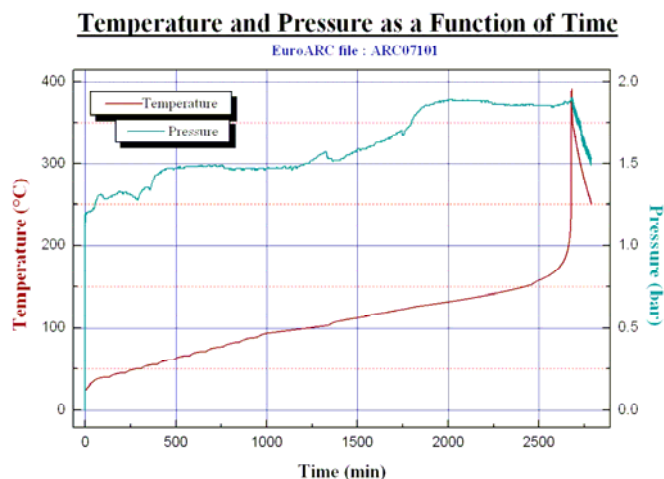


Figure 55. Temperature-time and temperature-pressure profiles of a commercially available lithium mixed oxide 18650 cell tested in the closed ARC configuration.

Table 4. Accelerating Rate Calorimetry summary results for the open and closed configurations.

	Open/Closed Configuration	Total Enthalpy (Joules)	Observed Onset Temp (T_o) °C	Self Heat Rate at T_o (M_o) °C/min	Temp at Maximum Rate (T_{mr}) _{sys} °C	Max. Self Heat Rate (M_{mr}) _{sys} °C/min	Final Adiabatic Temp (T_{ab}) _{sys} °C	Adiabatic Temp. Rise (D_{Tab}) _{sys} °C ($T_{ab}-T_o$)
Valence Phosphate								
15930498	Open	16495	83.1	0.121	300.9	12.3	406.1	322.9
15930323	Closed	21682	88.5	0.027	232.7	0.497	399.3	311.0
Commercial Lithium Cobalt Oxide								
1008670	Open	19583	81.7	0.034	433.0	5513.2	433.0	351.3
1008738	Closed	11075	83.5	0.021	225.1	126.9	242.6	159.1
Commercial Lithium Mixed Oxide								
2006456	Open	24713	80.1	0.027	405.2	2588.1	548.6	468.5
2009241	Closed	22260	88.2	0.021	307.6	124.3	388.4	300.3

The rate of temperature change as a function of temperature indicates the nature of the self-heating rate of the different Li-ion cell chemistries, as shown in Figure 56 to Figure 61. The self-heating rate is indicative of the energetic thermal decomposition of the cell. Valence phosphate chemistry showed a much lower self-heating rate (Figure 56) compared to either commercially available lithium cobalt oxide/mixed oxide 18650 cell chemistry tested (Figure 57 and Figure 58) in the open ARC configuration. In the closed ARC configuration, the rate of self-heating was expected to be lower than in the open configuration because of the loss of heat to the pressure vessel. The Valence phosphate cell showed a comparatively very low (less than

1 °C/min) self-heating rate, as shown in Figure 59. Additionally, there was no significant increase in rate of pressure development as expected since energetic thermal decomposition did not occur, as shown in Figure 59. Both commercially available lithium cobalt oxide/mixed oxide 18650 cell chemistries tested showed an increase rate of self-heating before energetic thermal decomposition, as shown in Figure 60 and Figure 61. Plots of the temperature change rate (self-heating rate) vs. temperature for the three different cell chemistries tested shown together indicate the relative self-heating rates in the open and closed ARC configurations, as shown in Figure 62 and Figure 63, respectively. In both open and closed configurations the Li-ion cell chemistries can be ranked from highest self-heating rate to lowest as follows: lithium cobalt oxide 18650 cells > lithium mixed oxide 18650 cells > Valence phosphate. The peak self-heating rate and temperature at which self-heating occurred are summarized in Table 4.

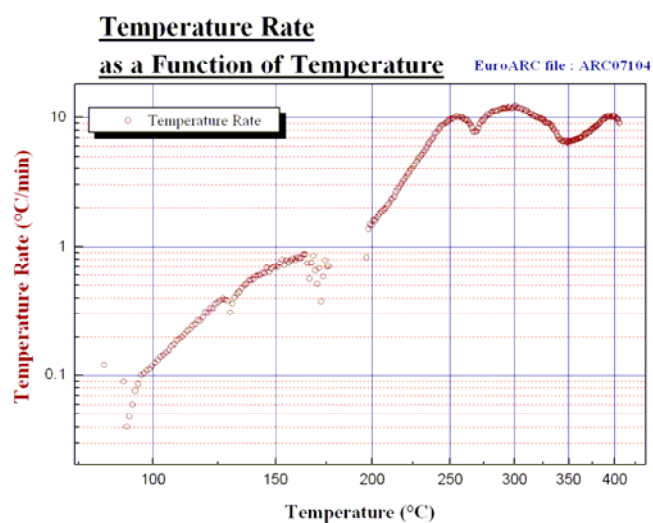


Figure 56. Temperature rate as a function of temperature for Valence phosphate 18650 cell tested in the open ARC configuration.

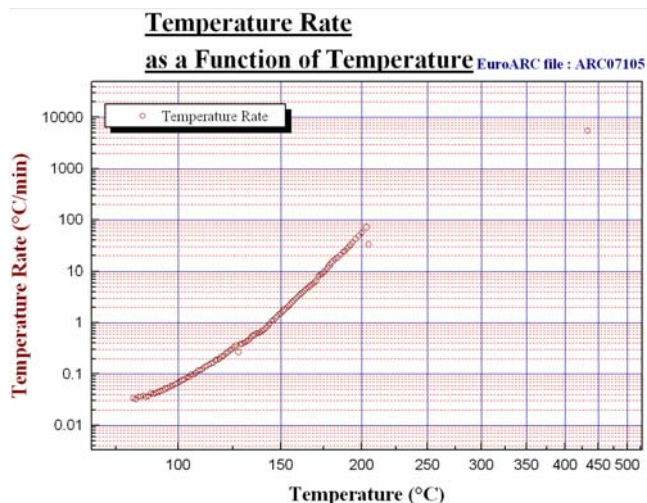


Figure 57. Temperature rate as a function of temperature for a commercially available lithium cobalt oxide 18650 cell tested in the open ARC configuration.

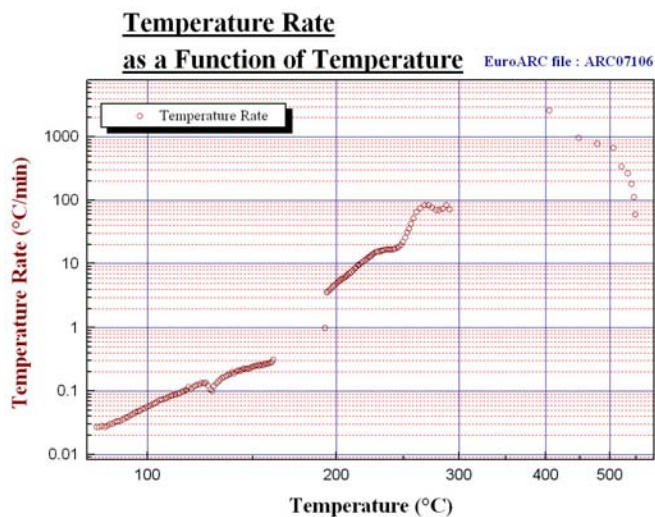


Figure 58. Temperature rate as a function of temperature for commercially available lithium mixed oxide 18650 cell tested in the open ARC configuration.

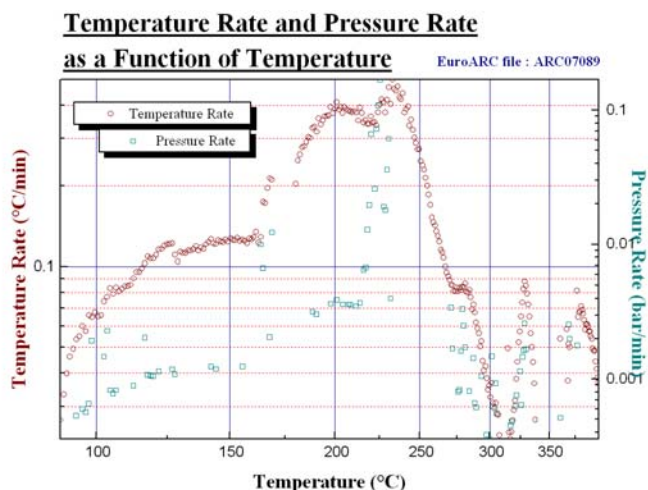


Figure 59. Temperature rate and pressure rate as a function of temperature for Valence phosphate 18650 cell tested in the closed ARC configuration.

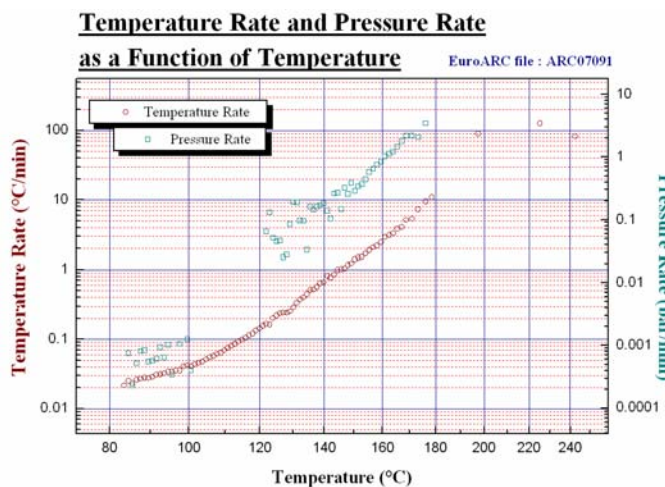


Figure 60. Temperature rate and pressure rate as a function of temperature for a commercially available lithium cobalt oxide 18650 cell tested in the closed ARC configuration.

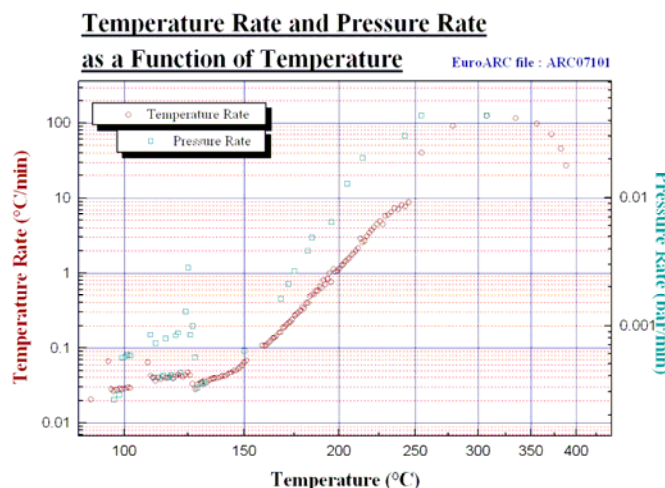


Figure 61. Temperature rate and pressure rate as a function of temperature for a commercially available lithium mixed oxide 18650 cell tested in the closed ARC configuration.

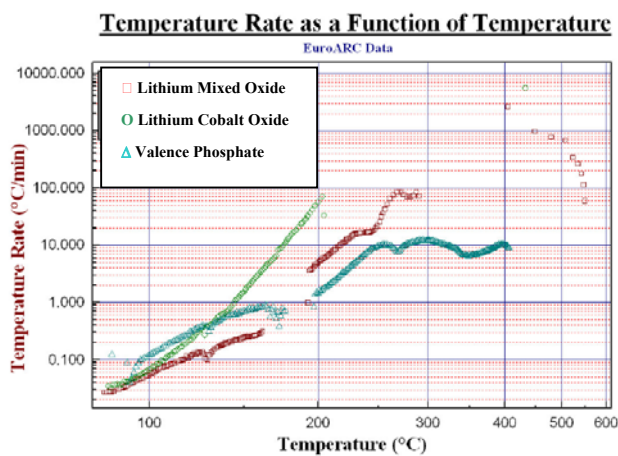


Figure 62. Temperature-time series comparison of Li-ion cell chemistries tested in ARC open configuration.

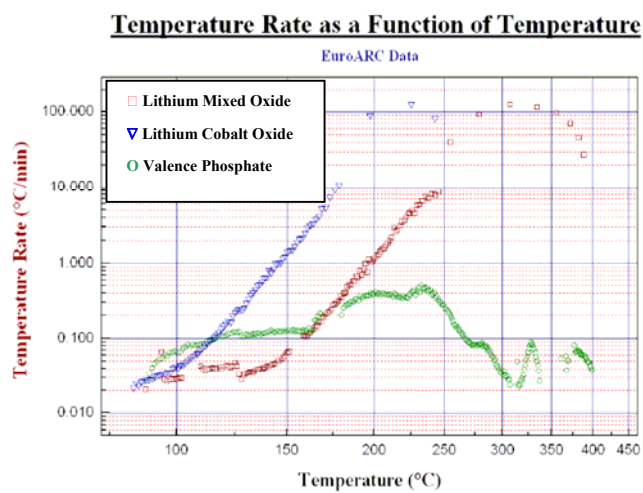


Figure 63. Temperature-time series comparison of Li-ion cell chemistries tested in ARC closed configuration

In the open ARC configuration the cell voltage was monitored throughout the duration of the experiments. The time and associated temperature can be noted at which the separator failure occurred as evident by the cell voltage drop. The voltage-time curves for the three different chemistries are shown in Figure 64 through Figure 66. Separator shutdown occurred between 120 and 150 °C in all the cell chemistries tested. Note that the separator failure occurred after the self-heating onset temperature in all cases, which is consistent with the generally accepted notion that self-heating is initiated at ~80 °C by SEI film breakdown in the anode.

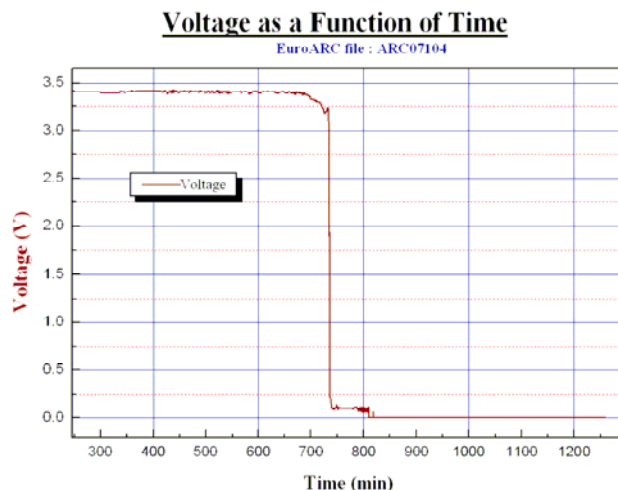


Figure 64. Voltage-time series of Valence phosphate 18650 cell tested in the open ARC configuration. A voltage drop was observed at approximately 150°C corresponding to the time at which breakdown was observed.

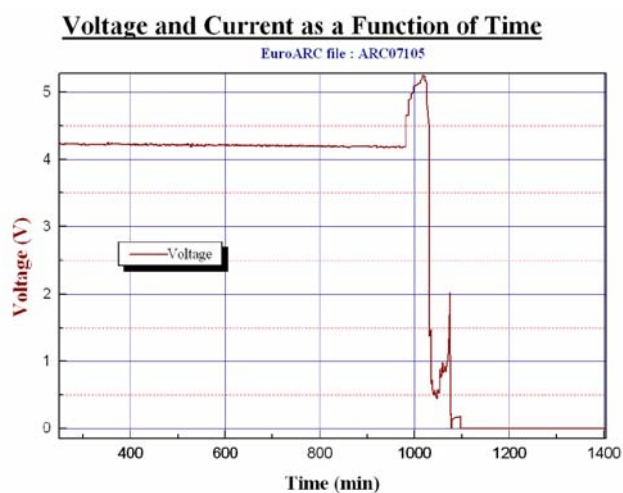


Figure 65. Voltage-time series of a commercially available lithium cobalt oxide 18650 cell tested in the open ARC configuration. A voltage drop was observed at approximately 120°C corresponding to the time at which breakdown was observed.

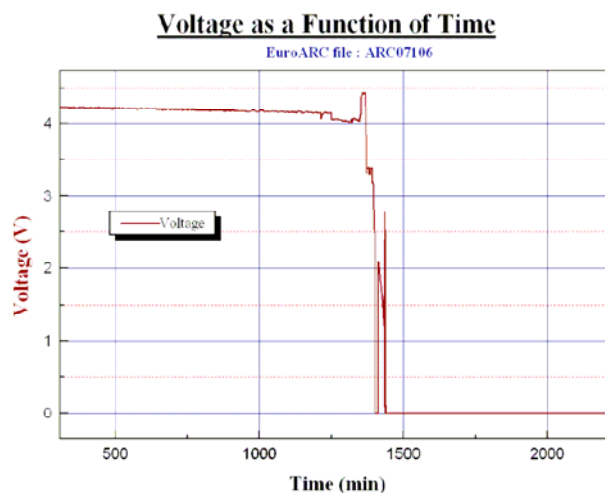


Figure 66. Voltage-time series of a commercially available lithium mixed oxide 18650 cell tested in the open ARC configuration. A voltage drop was observed at approximately 150°C corresponding to the time at which breakdown was observed.

Photographs of Li-ion cells were taken after ARC testing. In all cases the cells appeared to be burned, as shown in Figure 67 through Figure 73. Black residue was found in the ARC bomb in all cases after testing. In most cases, cells contained their cell windings and appear to have vented as intended. However, the commercially available lithium cobalt oxide 18650 cell tested underwent crimp failure resulting in the vent end of the cell separating from the rest of the cell can, as shown in Figure 72.



Figure 67. Photograph of Valence phosphate cell after ARC testing in the open configuration.



Figure 68. Photograph of Valence phosphate cell after ARC testing in the open calorimeter bomb apparatus.

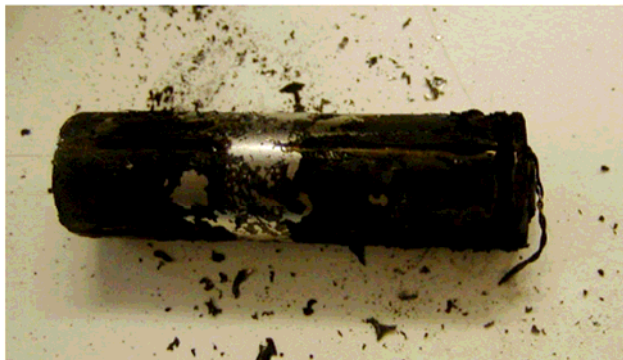


Figure 69. Photograph of a commercially available lithium cobalt oxide 18650 cell after ARC testing in the open cell configuration.



Figure 70. Photograph of a commercially available lithium mixed oxide 18650 cell after ARC testing in the open cell configuration.



Figure 71. Photograph of Valence phosphate cell after ARC testing in the closed configuration.



Figure 72. Photograph of a commercially available lithium cobalt oxide 18650 cell after ARC testing in the closed cell configuration.



Figure 73. Photograph of a commercially available lithium mixed oxide 18650 cell after ARC testing in the closed cell configuration.

Test Summary

The results of the Accelerating Rate Calorimetry testing indicate:

- The self-heating onset temperature was shown to occur between 80 °C and 90 °C for all cell chemistries tested.
- The peak temperatures achieved upon thermal runaway were between 245 °C and 550 °C.
- In both open and closed configurations the Li-ion cell chemistries tested can be ranked from highest self-heating rate to lowest as follows: commercially available lithium cobalt oxide 18650 cells > commercially available lithium mixed oxide 18650 cells > Valence phosphate.
- Separator shutdown occurs between 120 °C and 150 °C in all the cell chemistries tested.